The University of Manitoba

A PROTON MAGNETIC RESONANCE STUDY OF THE HINDERED ROTATION IN α,α,2,3,6-PENTACHLOROTOLUENE

by

Mark Andrew Halden Stewart

A Thesis

Submitted to

the Faculty of Graduate Studies and Research

University of Manitoba

in Partial Fulfillment

of the Requirements for the Degree

MASTER OF SCIENCE

Winnipeg, Manitoba

August, 1970

TO MY FAMILY

ACKNOWLEDGEMENTS

I would like to express my gratitude to Dr. T. Schaefer for the instruction and patient guidance he has shown me throughout the past year.

I also appreciate the direction given to me by Dr. H. Hutton.

The numerous discussions with my friends of the NMR lab, Brian Barber, Fred Janzen, Jim Peeling and Rod Wasylishen were exceedingly beneficial.

Finally, I am indebted to the University of Manitoba for financial assistance.

ABSTRACT

A high resolution proton magnetic resonance investigation of the hindered rotation of the dichloromethyl group in α, α, 2, 3, 6 - pentachlorotoluene has been conducted using a complete line-shape analysis of the experimental spectra. The rate process involved in the rotation consists of a nonmutual exchange of three pairs of protons between two unequally populated conformations. The activation parameters were determined from a computational treatment of the experimental spectra over a temperature range from 255°K to 378°K. The Arrhenius activation energy for a 20 mole % solution of α, α, 2, 3, 6 - pentachlorotoluene has a calculated value of 14.0±0.3 Kcal $mole^{-1}$. Treatment of the data using the absolute reaction rate theory provided values for the free energy of activation (15.4±0.1 Kcal $mole^{-1}$ at 298°K), the enthalpy of activation (13.3±0.3 Kcal $mole^{-1}$) and the entropy of activation (-7.0±0.7 eu). The results are compared with those of analogous molecules.

TABLE OF CONTENTS

CHAPTER		PAGE
I	INTRODUCTION	1
II	THEORETICAL DISCUSSION	4
	A. Classical Line-shape Theories	5
	1. Relaxation and the Bloch Equations	5
	2. Classical Exchange Theory	7
	B. Quantum Mechanical Line-shape Theory	8
	C. Determination of Activation Parameters	11
III	NATURE OF THE PROBLEM	13
IV	EXPERIMENTAL	15
	A. Preparation of α, α, 2, 3, 6 - Pentachlorotoluene Solution	16
	B. Proton Magnetic Resonance Measurements	17
V	RESULTS AND DISCUSSION	18
	A. General Appearance of Spectra at Various Temperatures	19
	B. Conformational Assignment at Low Temperatures	34
	C. Proton Assignments	39
	1. Proton Assignment of High Temperature Spectra	39
	2. Proton Assignment of Low Temperature Spectra	42
	D. Rationalization of the Chemical Shifts	53
	1. In the Absence of the Dichloromethyl Group	53
	(a) Substituent Effect	53
	(b) Solvent Effect	54

2. In the Presence of the Dichloromethyl Group .. 55

(a) Steric Effects 55

(b) Solvent Effects 57

(c) Dipole Moments 58

(d) Summary 58

E. Relative Populations of the Two Conformations .. 61

1. Low Temperature Populations 61

2. High Temperature Populations 63

(a) The Assumption 63

(b) The Justification 63

F. The Rate Process 66

1. Determination of Rate Constants 66

(a) Computer Program DNMR 66

(b) Effective Transverse Relaxation Time 66

(c) Solvent Effects 67

2. Calculation of the Activation Parameters 75

3. Errors 99

G. Summary and Conclusions 101

H. Suggestions for Future Research 103

BIBLIOGRAPHY 104

LIST OF TABLES

TABLE		PAGE
I	Chemical shifts, coupling constants and linewidths of the ring protons at temperatures above the coalescence temperature	40
II	Chemical shifts and coupling constants for the protons of conformation I at temperatures below the coalescence temperature	47
III	Chemical shifts and coupling constants for the protons of conformation II at temperatures below the coalescence temperature	48
IV	Chemical shifts of the four possible assignments ...	51
V	Relative intensities of the $H_{X(I)}$ and $H_{X(II)}$ peaks in the low temperature region	62
VI	Relative intensities of the AB(I) quartet to the AB(II) quartet in the low temperature region	62
VII	The calculated ASIS for the average line position of A(I) and A(II) (i.e. δ_A) and the average line position of B(I) and B(II) (i.e. δ_B).....	69
VIII	Calculated ASIS for the separation between B(I) and B(II) (i.e. $\delta_{B(I)B(II)}$) and A(I) and A(II) (i.e. $\delta_{A(I)A(II)}$).....	71
IX	Calculated values for the chemical shifts of the ring protons of 2, 3, 6 - PCT.....	74

X Rate constants at various temperatures 76

XI Summary of the activation parameters for 2, 3, 6 - PCT in toluene-d_8, for OCX and for PCT 94

LIST OF FIGURES

FIGURE		PAGE
1.	The PMR spectrum of a 20 mole % solution of 2, 3, 6 - PCT in toluene-d_8 at 254.6°K	22
2.	The PMR spectrum of a 20 mole % solution of 2, 3, 6 - PCT in toluene-d_8 at 275.7°K	25
3.	The PMR spectrum of a 20 mole % solution of 2, 3, 6 - PCT in toluene-d_8 at 286.3°K	27
4.	The PMR spectrum of a 20 mole % solution of 2, 3, 6 - PCT in toluene-d_8 at 298.8°K	29
5.	The PMR spectrum of a 20 mole % solution of 2, 3, 6 - PCT in toluene-d_8 at 320.1°K	31
6.	The PMR spectrum of a 20 mole % solution of 2, 3, 6 - PCT in toluene-d_8 at 378.2°K	33
7(a).	Incorrect conformational assignment at low temperatures	38(a)
7(b).	Correct conformational assignment at low temperatures .	38(b)
8.	High temperature chemical shifts versus 1/T	44
9.	A plot of δ_{AB} versus 1/T	46
10.	The four possible proton assignments at low temperatures	50
11.	Chemical shifts of the ring protons versus 1/T	73
12.	Experimental and calculated PMR spectra of a 20 mole % solution of 2, 3, 6 - PCT in toluene-d_8 at 254.6°K ...	78
13.	Experimental and calculated PMR spectra of a 20 mole % solution of 2, 3, 6 - PCT in toluene-d_8 at 275.7°K	80

14. Experimental and calculated PMR spectra of a 20 mole % solution of 2, 3, 6 - PCT in toluene-d_8 at 286.3°K ... 82

15. Experimental and calculated PMR spectra of a 20 mole % solution of 2, 3, 6 - PCT in toluene-d_8 at 298.8°K 84

16. Experimental and calculated PMR spectra of a 20 mole % solution of 2, 3, 6 - PCT in toluene-d_8 at 320.1°K 86

17. Experimental and calculated PMR spectra of a 20 mole % solution of 2, 3, 6 - PCT in toluene-d_8 at 378.2°K 88

18. Eyring plot of log k/T versus 1/T 91

19. Arrhenius plot of log k versus 1/T 93

20. A graphical representation of the free energy change for the hindered rotation in 2, 3, 6 - PCT 96

CHAPTER I

INTRODUCTION

Steady state nuclear magnetic resonance (NMR) spectroscopy is a particularly versatile technique when applied to the study of molecular and electronic motions such as hindered rotation about bonds, ring inversions and proton exchanges. It is most useful for the study of rate processes between states of thermodynamic equilibrium involving a barrier of between 5 and 25 Kcal $mole^{-1}$.

Line-shapes of NMR spectra are frequently sensitive to the rate of the process. If the rate is a function of some experimental parameter which can be easily varied, such as temperature or pH, then the process is amenable to study by the NMR technique. The advent of the high speed computer has made a complete quantum mechanical treatment of the NMR line-shapes possible. Hence, a comparison of the experimental and calculated NMR spectra can yield detailed knowledge of the rate process. Several comprehensive reviews on this method of analysis are available in the literature (1-5).

This thesis deals specifically with the application of NMR to the investigation of the rate process involved in the hindered rotation of the dichloromethyl group in α, α, 2, 3, 6 - pentachlorotoluene (2, 3, 6 - PCT). The rate constants were obtained by fitting the experimental

spectra to the computer-simulated spectra calculated from a complete quantum mechanical treatment of the exchange process. The activation parameters were calculated from both the Arrhenius and absolute reaction rate theories. Discussion on the proton assignments, the solvent shifts and the populations is given in detail in chapter V. As well, an assessment of the activation parameters is made by comparison with analogous molecules.

CHAPTER II

THEORETICAL DISCUSSION

A. Classical Line-Shape Theories

1. Relaxation and the Bloch Equations

In an external magnetic field $\underline{H}$ a nucleus with spin angular momentum $|\underline{I}| = \frac{h}{2\pi}\{I(I+1)\}^{\frac{1}{2}}$ and magnetic moment $\underline{\mu} = \gamma\underline{I}$ precesses with frequency $\omega_o = \gamma H$ about the direction of the magnetic field (conventionally the z direction) according to the equation,

$$\frac{d\underline{\mu}}{dt} = \gamma(\underline{\mu} \times \underline{H}) . \qquad (2\text{-}1)$$

When a number of magnetic nuclei are assembled in an external magnetic field all of the magnetic dipoles precess about the direction of the magnetic field in random phase. The x and y components of the resultant macroscopic magnetization $\underline{M}$ are therefore zero and the only non-zero component is along the z direction.

If the assembly of magnetic dipoles is subjected to a secondary magnetic field H_1 oscillating at frequency ω in the same direction as the precessional motion in the xy plane, then a certain degree of in phase precessional motion results. The x and y components of $\underline{M}$ become different from zero and the resultant macroscopic magnetization vector precesses according to the equation,

$$\frac{d\underline{M}}{dt} = \gamma(\underline{M} \times \underline{H}). \qquad (2\text{-}2)$$

Relative to a frame of reference rotating about the z axis

with frequency ω, the components of equation (2-2) can be written as

$$\frac{dM_x}{dt} = (\omega_o - \omega)\, M_y \qquad (2\text{-}3)$$

$$\frac{dM_y}{dt} = -(\omega_o - \omega)\, M_x + \gamma H_1\, M_z \qquad (2\text{-}4)$$

$$\frac{dM_z}{dt} = -\gamma\, H_1\, M_y \qquad (2\text{-}5)$$

The NMR experiment involves the detection of changes in the macroscopic magnetization in the xy plane. It is therefore convenient to define the complex xy magnetization G by the equation,

$$G = M_x + iM_y \,. \qquad (2\text{-}6)$$

Using equation (2-6) to combine equations (2-3) and (2-4) one obtains,

$$\frac{dG}{dt} = -i(\omega_o - \omega)G + i\,\gamma H_1 M_z. \qquad (2\text{-}7)$$

To complete the description of the time-dependent behaviour of the macroscopic magnetization the interactions of the magnetic nuclei with their environment must be considered. Such interactions are collectively referred to as relaxation processes. According to Bloch (6) such processes can be described by first-order rate processes characterized by the relaxation times T_1 and T_2. Equations (2-5) and (2-7) can be modified to take the relaxation phenomena into

account to give the complete Bloch equations,

$$\frac{dG}{dt} = -i(\omega_o - \omega)G + i\gamma H_1 M_z - \frac{1}{T_2} G \qquad (2\text{-}8)$$

$$\frac{dM_z}{dt} = -\gamma H_1 M_y - \frac{1}{T_1}(M_z - M_o), \qquad (2\text{-}9)$$

where M_o is the equilibrium value of M.

2. Classical Exchange Theory

The early attempts to develop a theoretical framework for the exchange phenomenon were all based on the Bloch equations (7-11). Bloch's description of the NMR experiment presumes a system of independent spins and therefore can not be expected to apply in the case of a coupled system. Because of their limited applicability, analysis of lineshapes using the Bloch equations is now considered obsolete.

B. Quantum Mechanical Line-Shape Theory

The limited scope of the approximations used in the derivations of classical line-shape theory greatly restricts their usefulness and validity. A quantum mechanical approach based on the density matrix formalism was initiated by Kaplan (12) and further developed by Alexander (13) and Whitesides (14). Binsch (15) developed the theory in the Liouville representation of quantum mechanics rather than in the Hilbert space representation. A brief presentation of the quantum mechanical treatment of an exchanging system is now given using the AB system as a specific example.

Consider the situation where x identical coupled nuclei of spin ½ are located in n different magnetic environments. In order to calculate the line-shape of the NMR spectrum when the nuclei begin to exchange, it is necessary to first evaluate the total transverse magnetization, G (see equation 2-6). Each magnetic environment m can be described by a state function ψ_m which can be expanded in terms of a complete set of orthonormal spin basis functions ϕ_i,

$$\psi_m = \sum C_{mi}\, \phi_i \,. \qquad (2 - 10)$$

G can be determined from the equation,

$$G = \sum_m P_m\, G_m \qquad (2 - 11)$$

where P_m is the population of the spin system in magnetic environment m, and

$$G_m = \frac{\gamma}{2\pi} \langle I^- \rangle \tag{2-12}$$

is the expectation value of the operator $\frac{\gamma I^-}{2\pi}$, where I^- is the lowering operator.

By combining equations (2-10) and (2-12) one obtains

$$\begin{aligned} G_m &= \frac{\gamma}{2\pi} \sum_{ij} \langle \phi_i | I^- | \phi_j \rangle \rho^m_{ji} \\ &= \frac{\gamma}{2\pi} \mathrm{Tr}(I^- \rho^m) \end{aligned} \tag{2-13}$$

where $\rho^m_{ji} = c_{mj} c^*_{mi}$ are the elements of the density matrix for the m^{th} magnetic environment. For an AB system the spin basis functions are generally chosen to be $\alpha\alpha, \alpha\beta, \beta\alpha$ and $\beta\beta$. Using this expansion set, one obtains

$$I^- = \begin{bmatrix} 0 & 0 & 0 & 0 \\ 1 & 0 & 0 & 0 \\ 1 & 0 & 0 & 0 \\ 0 & 1 & 1 & 0 \end{bmatrix} . \tag{2-14}$$

Substitution of equation (2-14) into (2-13) gives

$$G_m = \frac{\gamma}{2\pi} (\rho^m_{12} + \rho^m_{13} + \rho^m_{24} + \rho^m_{34}) \tag{2-15}$$

for the AB case.

In the presence of relaxation and exchange the equation of motion is

$$\frac{d\rho^m}{dt} = 2\pi i \left[\rho^m, \mathcal{H}^m\right] + \left(\frac{d\rho^m}{dt}\right)_{\text{relax.}} + \left(\frac{d\rho^m}{dt}\right)_{\text{exch.}} \tag{2-16}$$

$$= 2\pi i \left[\rho^m, \mathcal{H}^m\right] - \frac{\rho^m}{T_{2m}} + \sum_{l \neq m} (k_{lm}\, \rho^l - k_{ml}\, \rho^m) \qquad (2\text{-}16)$$

where $\mathcal{H}^m$ is the standard high-resolution spin Hamiltonian expressed in frequency units,

k_{lm}, k_{ml} are the first order rate constants for the forward and reverse exchanges, and

T_{2m} is the transverse relaxation time.

Under steady state, unsaturated conditions the left-hand sides of equations (2-16) become zero and a set of linear equations for ρ^m_{ij} is obtained. Once the elements ρ^m_{ij} are known, G_m and G can be readily evaluated from (2-15) and (2-11) and the line-shape of the NMR spectra for different rate constants can be determined.

C. Determination of Activation Parameters

From a linear plot of the Arrhenius equation,

$$\ln k = - E_a/RT + \ln A, \qquad (2\text{-}17)$$

one can determine a value for the activation energy E_a. from the slope, and for the frequency factor A from the intercept. The usefulness of such a plot is questionable, however, because it presupposes that E_a and A are temperature independent.

The Eyring equation,

$$k = \frac{\kappa k_b}{h} \exp(-\Delta G^{\neq}/RT), \qquad (2\text{-}18)$$

where κ is the transmission coefficient,

k_b is Boltzmann's constant, and

h is Planck's constant

can be used to estimate the free energy of activation $\Delta G^{\neq}$ from a single rate constant at the coalescence temperature.

Better values for the activation parameters can be obtained if the rate constants for several temperatures are known. Substitution of the expression,

$$\Delta G^{\neq} = \Delta H^{\neq} - T\Delta S^{\neq} \qquad (2\text{-}19)$$

into equation (2-18) and taking the logarithms of both sides gives

$$\ln (k/T) = (-\Delta H^{\neq}/R)\ 1/T + \ln (\kappa k_b/h) + \Delta S^{\neq}/R \ . \qquad (2\text{-}20)$$

Hence a plot of ln(k/T) versus 1/T gives a slope and intercept proportional to the enthalpy of activation $\Delta H^{\neq}$ and the entropy of activation $\Delta S^{\neq}$ respectively.

For the case involving exchange between two unequally populated sites the activation parameters for the forward and reverse directions are not equal. The ratio of the rate constants for the forward and reverse directions are inversely related to the ratio of the populations for the two sites,

$$k_{AB} P_A = k_{BA} P_B, \qquad (2\text{-}21)$$

where the symbols have their usual meaning. If the populations of the two sites are known, the activation parameters for both directions can be readily calculated.

CHAPTER III

NATURE OF THE PROBLEM

The purpose of this investigation is to determine the activation parameters associated with the internal hindered rotation of the dichloromethyl group in α,α,2,3,6 - pentachlorotoluene. At 254.6°K the dichloromethyl group is locked in one of two positions with the two methyl chlorines straddling one of the two ortho chlorines. The corresponding NMR spectrum at this temperature consists of two independent ABX spectra where the AB parts belong to the ring protons and the X parts belong to the methine protons. As the temperature is increased the dichloromethyl group begins to rotate and the corresponding protons of the two ABX spectra begin to exchange. Further increases in temperature result in the X protons coalescing firstly, the A protons secondly, and the B protons finally. At 378.2°K all the peaks have coalesced and sharpened producing a simple ABX spectrum.

By visually comparing the experimental spectra with computer-calculated spectra the rate constants at the various temperatures are determined. The study is further complicated by population differences between the two conformations, temperature dependent solvent shifts, and difficulties in proton assignments.

CHAPTER IV
EXPERIMENTAL

A. Preparation of α, α, 2, 3, 6 - Pentachlorotoluene Solution *

Five grams of 2, 3, 6 - trichlorotoluene were dissolved in 50 ml. of carbon tetrachloride in a cylindrical quartz flask. The solution was irradiated with a Hanovia ultraviolet lamp while chlorine gas was bubbled through the solution via a gas dispersing tube. The progress of the reaction was monitored by PMR, and the chlorination was continued until the spectrum no longer indicated the presence of the methylene protons of the tetrachloro intermediate at 5.12 ppm. The product was purified by vacuum sublimation.

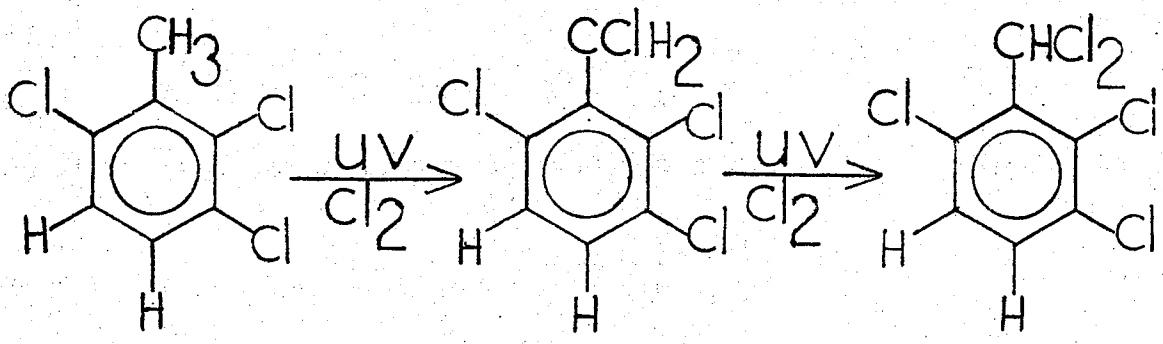

An approximate 20 mole % solution of α, α, 2, 3, 6 - pentachlorotoluene in toluene-d_8 was prepared and a small amount of TMS added. The solution was degassed using the freeze-pump-thaw technique. The sealed tube was tested for breakage up to 115°C in an oil bath.

* Thanks go to Mr. K. Chum, Summer Student, 1969, for this preparation.

B. Proton Magnetic Resonance Measurements

The proton magnetic resonance (PMR) spectra were obtained at 60 MHz with a Varian DA-60-I spectrometer equipped with a Varian V 4343 variable-temperature controller and at 100 MHz with a Varian HA 100 spectrometer equipped with a Varian V 6040 variable-temperature controller. The spectra were recorded with the spectrometers operating in the frequency sweep mode and locked to internal TMS.

The spectra of 2, 3, 6 - PCT at each temperature were recorded three to six times at a sweep rate of 0.02 or 0.05 Hz/sec keeping the amplitude of the rf. field and filtering at a minimum. The line positions were calibrated using period averaging techniques.

Each temperature was calibrated from the internal shift of ethylene glycol ($T>15^{o}C$) or methanol ($T<15^{o}C$) immediately before and after each run and is accurate to $\pm 1^{o}K$.

CHAPTER V

RESULTS AND DISCUSSION

A. General Appearance of Spectra at Various Temperatures

According to the rotational energy barrier calculations carried out recently by Barber (16), α, α, 2, 3, 6 - pentachlorotoluene (2, 3, 6 - PCT) at low temperatures (-20°C) exists in two rotational conformations. These rotamers are related by a 180° internal rotation of the dichloromethyl group and are shown below:

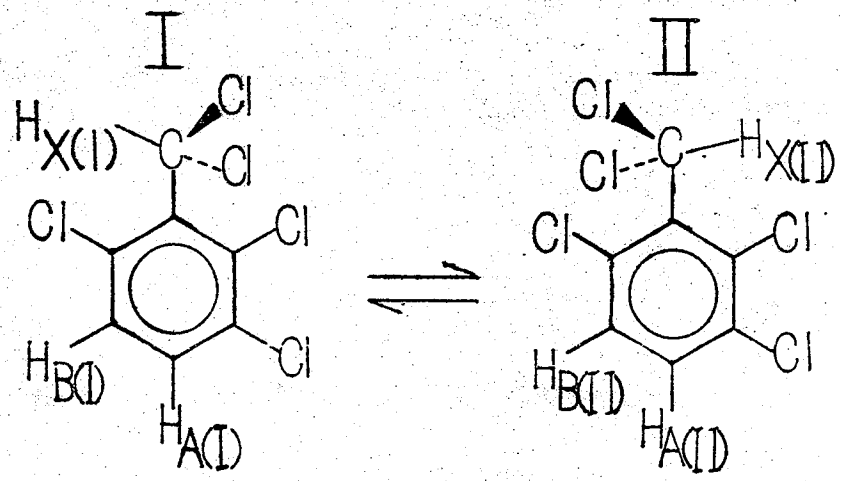

This 180° rotation effectively changes the magnetic environment of each proton. In the low temperature region where the lifetimes of the two conformations are long, the proton magnetic resonance spectra (PMR) of 2, 3, 6 - PCT show a significant chemical shift between the corresponding protons of each rotamer. Hence, PMR spectra in this temperature range consist of two independent ABX systems originating from the two independent rotamers. A typical low temperature spectrum of 2, 3, 6 - PCT is shown at the bottom of figure 1.

The aromatic portion of this spectrum shows two AB quartets, one with an internal chemical shift ($\delta_{A(I)B(I)}$) of 10.41 Hz and the other with an internal shift ($\delta_{A(II)B(II)}$) of 2.54 Hz. (See table II, section C). The shift between the two methine protons $H_{X(I)}$ and $H_{X(II)}$ is very small at this temperature and as a result the two peaks are very nearly superimposed. Above the experimental spectrum in figure 1 is a schematic representation of it. Included in the diagram is the correct conformational assignment of the two quartets as well as the correct assignment of the individual peaks. A complete description of how these assignments were made is given in sections B and C of this chapter.

If the rotation of the dichloromethyl group completes a 180° arc, $H_{A(I)}$ and $H_{A(II)}$, as well as $H_{B(I)}$ and $H_{B(II)}$, have effectively exchanged sites. The rate of these exchanges increases with increases in temperature producing dramatic changes in the appearance of the PMR spectra. The peaks belonging to the corresponding protons of each rotamer begin to broaden and move together. When the rate of exchange is of the same order of magnitude as the frequency separation in the absence of exchange, the peaks coalesce and a single broad absorption peak results. Typical spectra illustrating the line shapes of 2, 3, 6 - PCT just before and after coalescence are shown in figures 2, 3, and 5. Figure 4

FIGURE 1

The PMR spectrum of a 20 mole % solution of 2, 3, 6 - PCT in toluene-d_8 at 254.6°K.

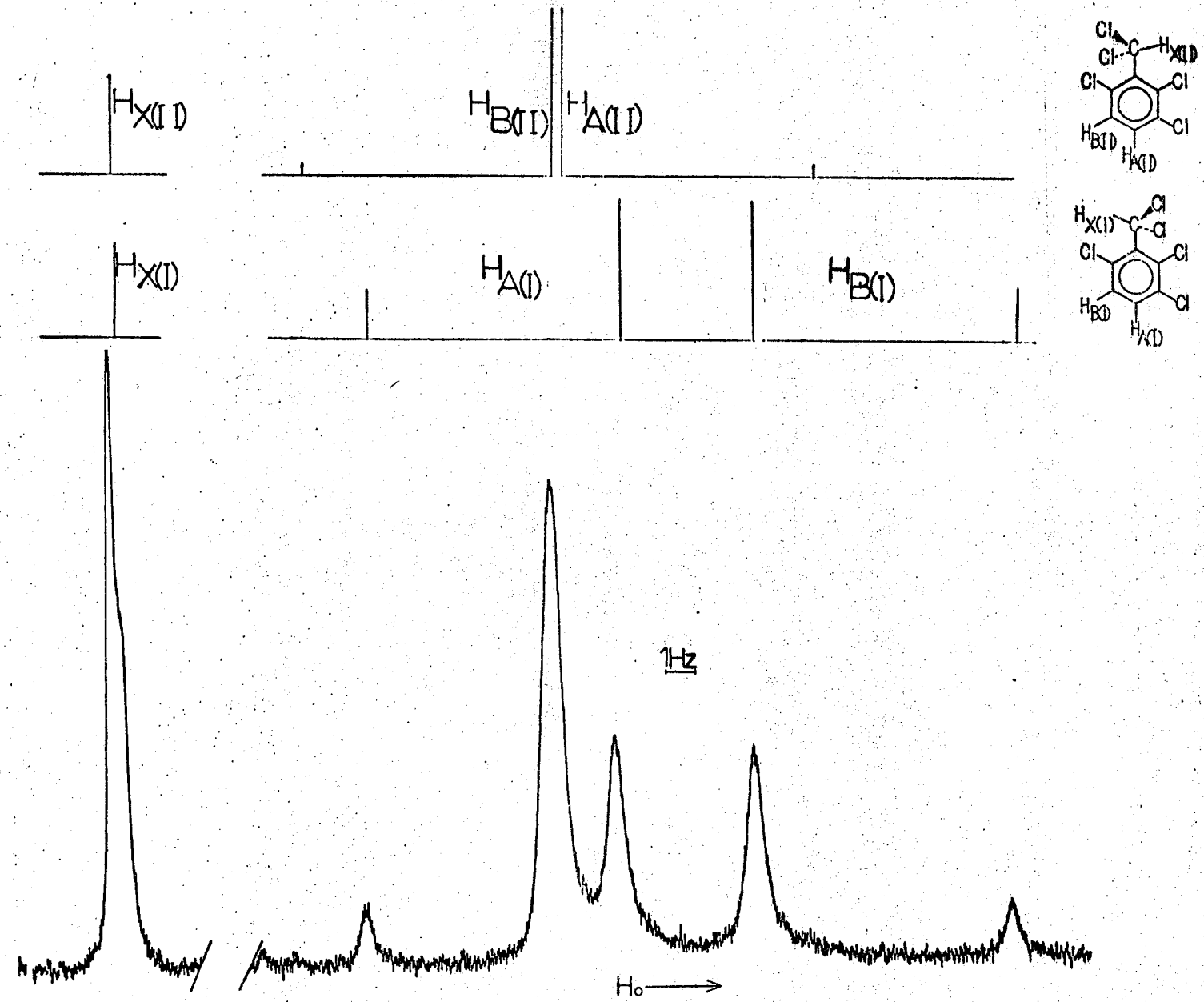
$H_{X(II)}$
$H_{B(II)}$
$H_{A(II)}$
$H_{X(I)}$
$H_{A(I)}$
$H_{B(I)}$
1Hz
H_o

illustrates the line shape at coalescence.

Further increases in the rate of exchange cause a sharpening of the broad peaks. When the rate of exchange is sufficiently rapid, the exchanging protons experience the same average magnetic environment and a simple ABX spectrum is observed. The limiting case is obtained when the line width is independent of the exchange process. A typical high temperature spectrum has been reproduced in figure 6.

FIGURE 2

The PMR spectrum of a 20 mole % solution of 2, 3, 6 - PCT in toluene-d_8 at 275.7°K.

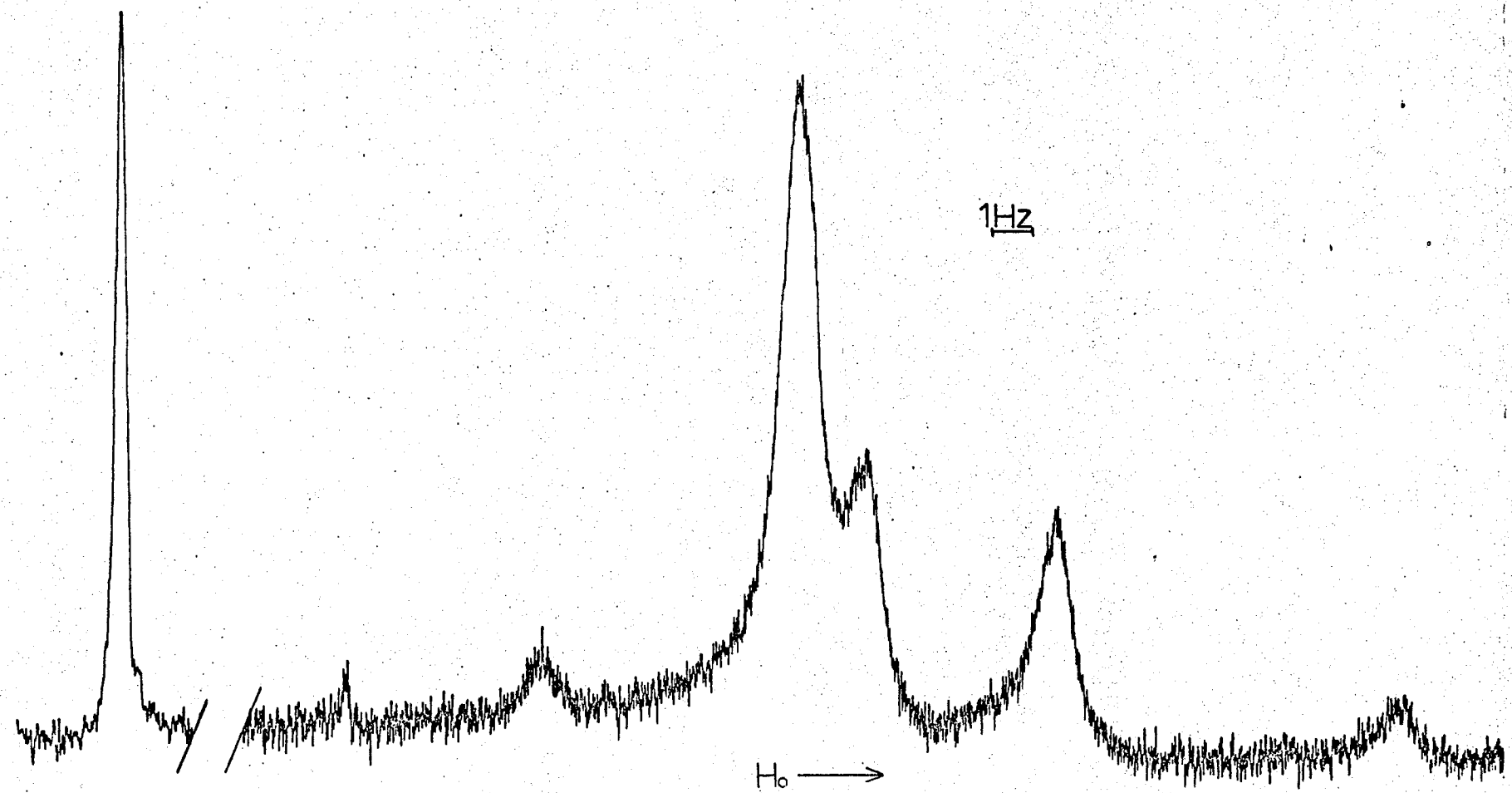
1Hz
H₀

FIGURE 3

The PMR spectrum of a 20 mole % solution of 2, 3, 6 - PCT in toluene-d_8 at 286.3°K.

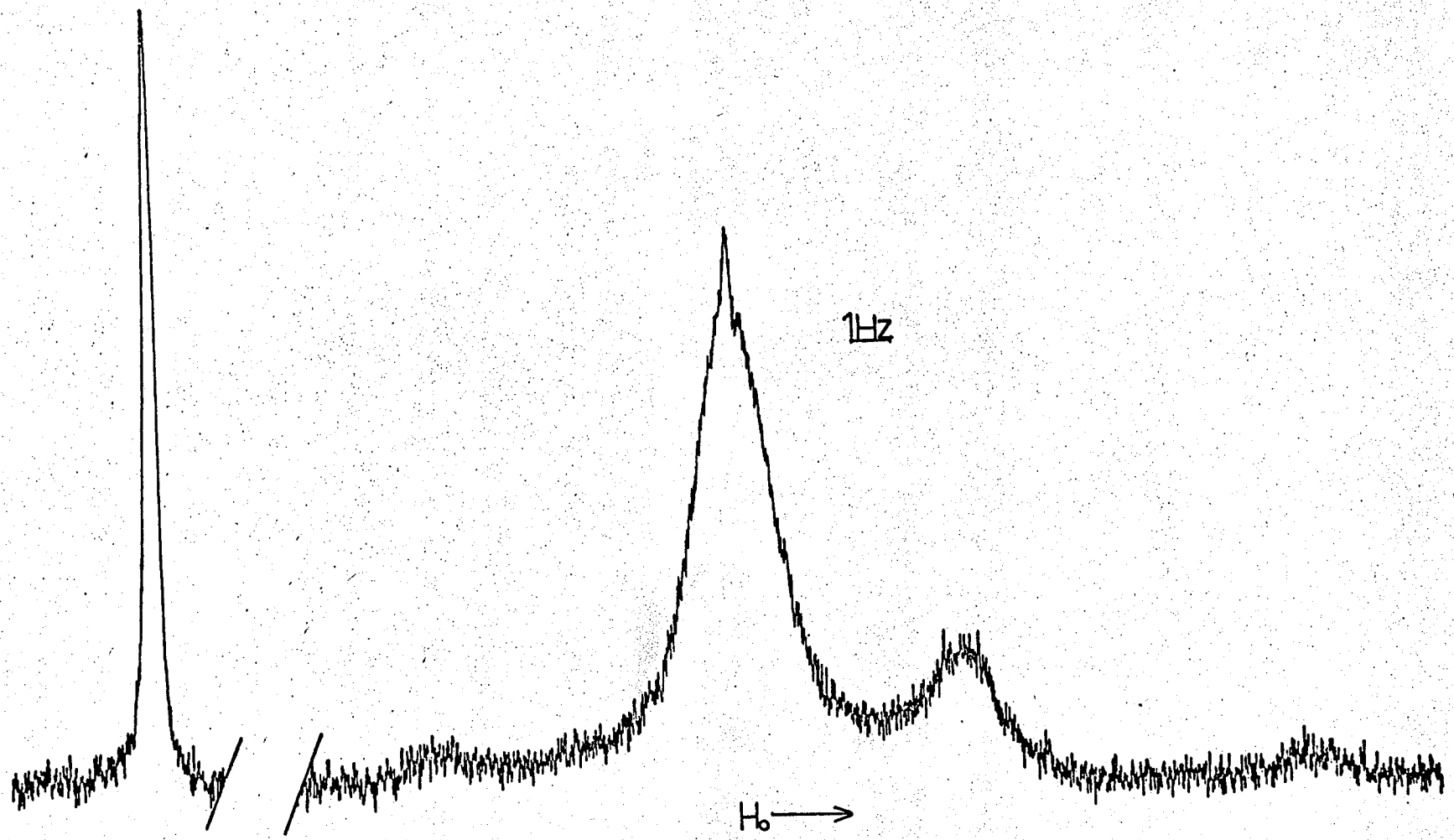
1Hz
H_0

FIGURE 4

The PMR spectrum of a 20 mole % solution of 2, 3, 6 - PCT in toluene-d_8 at 298.8°K.

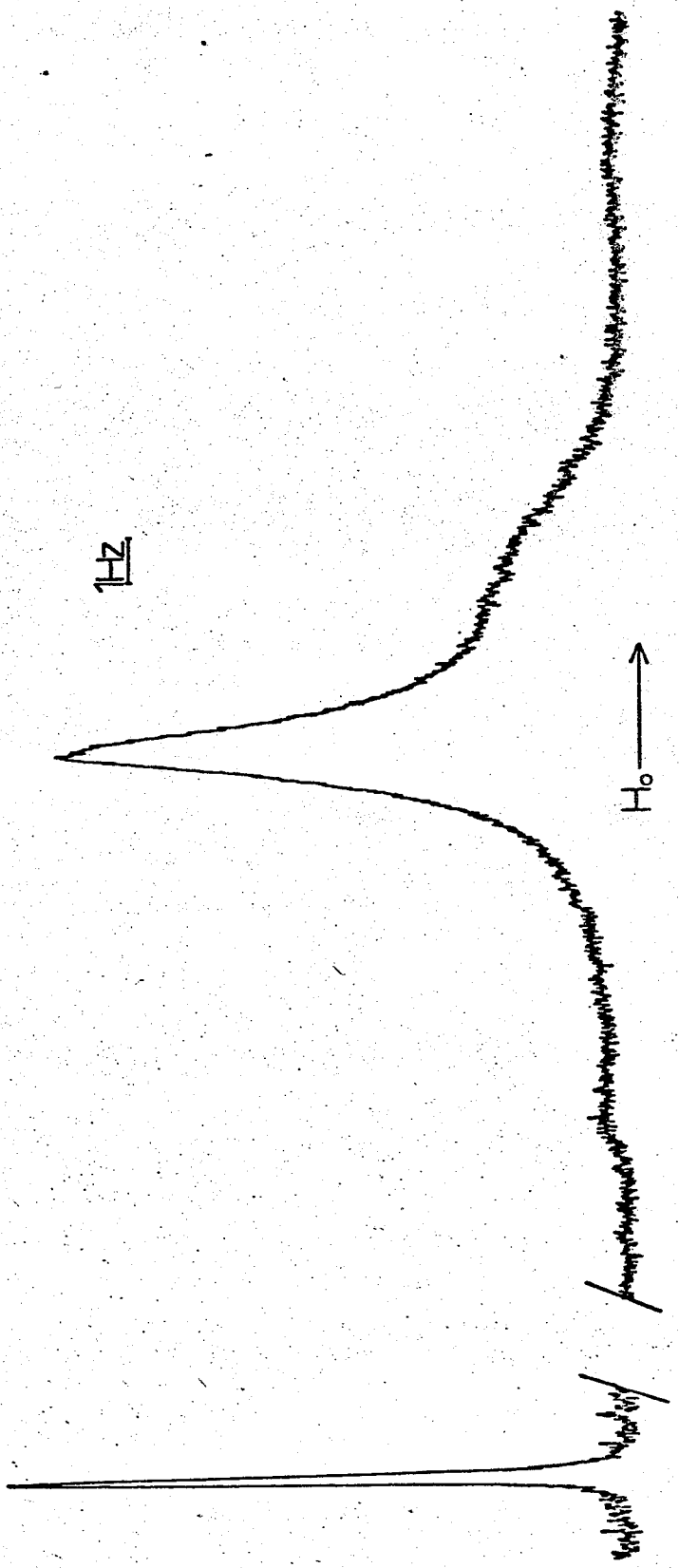
dH
H°

FIGURE 5

The PMR spectrum of a 20 mole % solution of 2, 3, 6 - PCT in toluene-d_8 at 320.1°K.

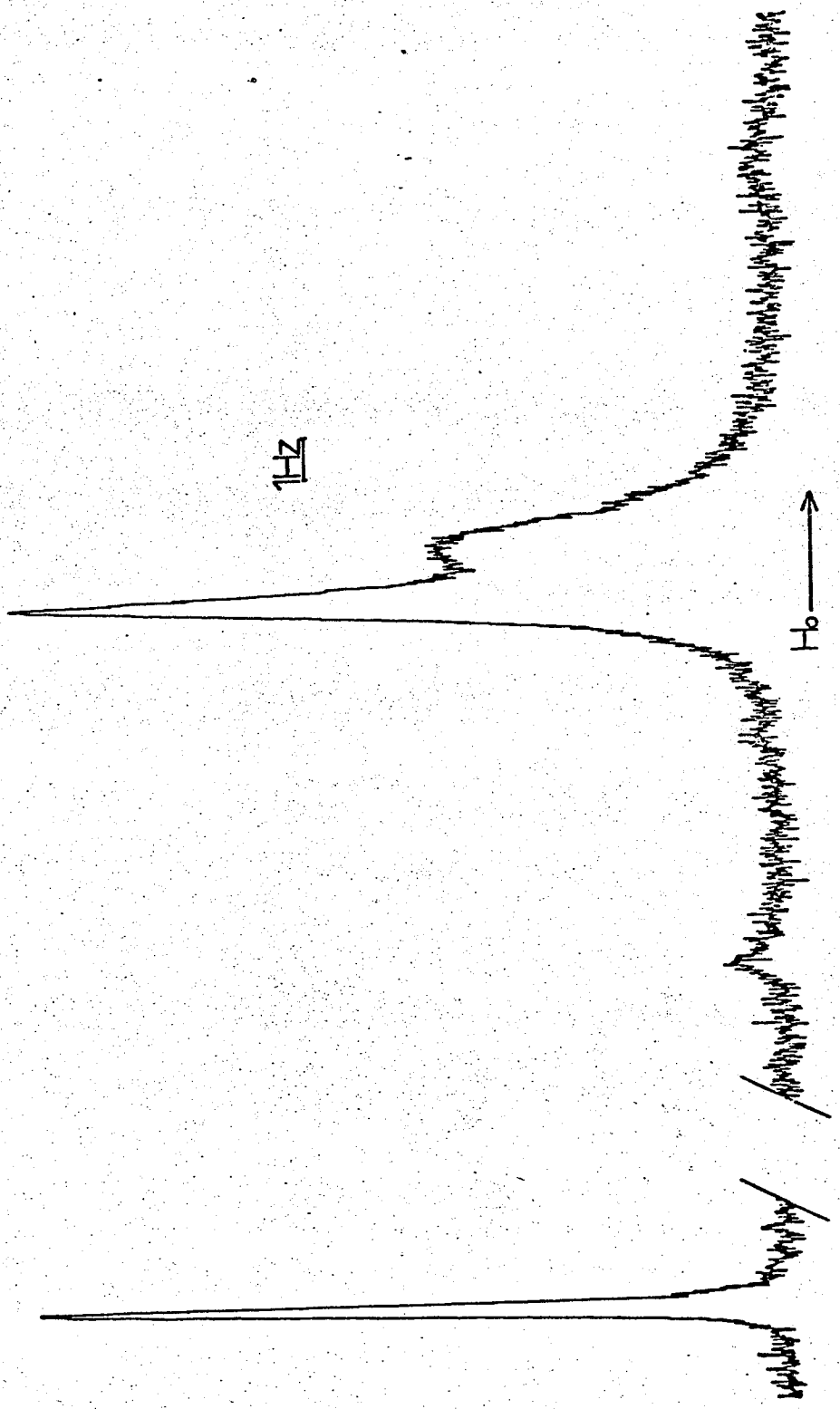
1H
H₀

FIGURE 6

The PMR spectrum of a 20 mole % solution of 2, 3, 6 - PCT in toluene-d_8 at 378.2°K.

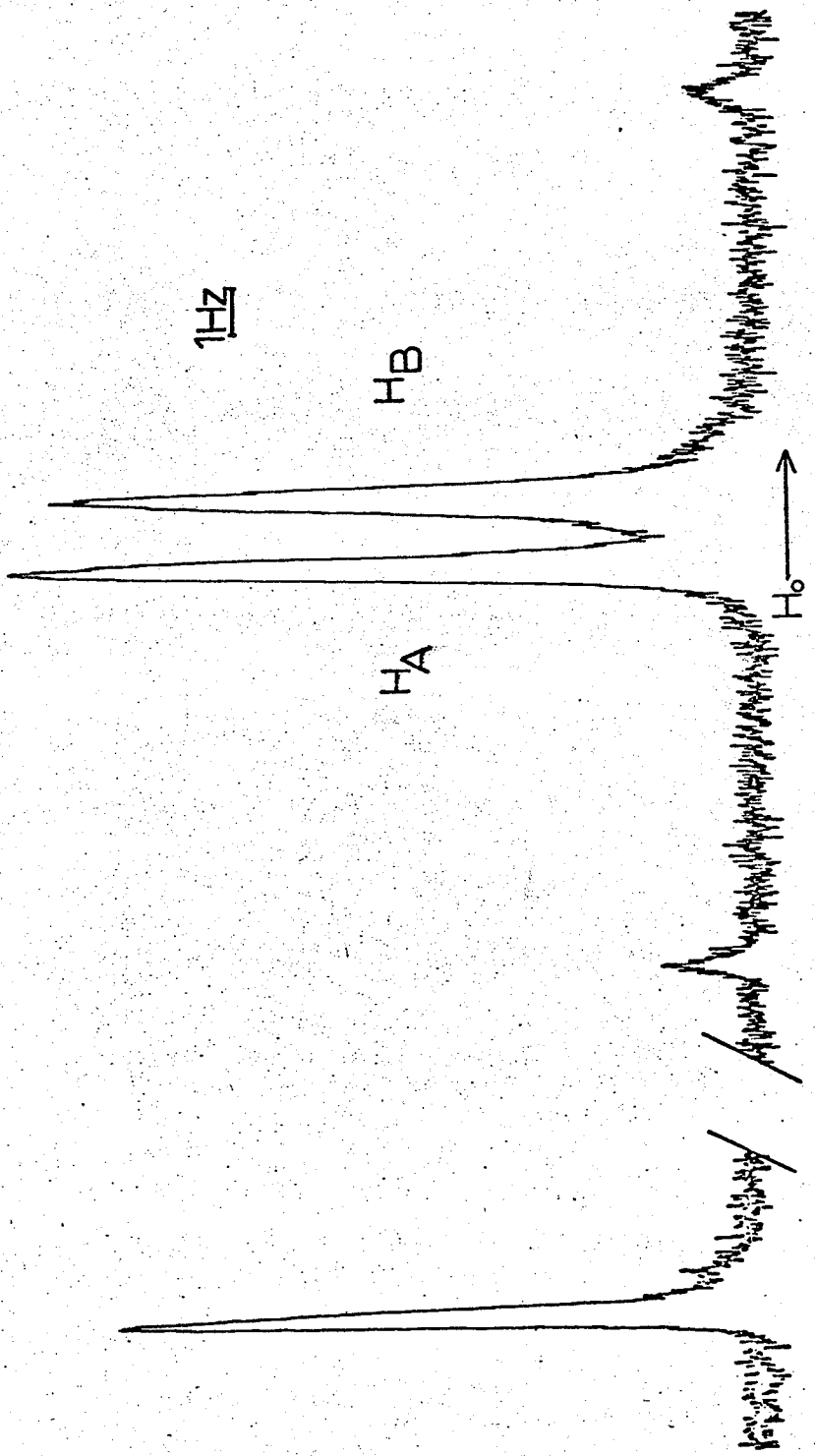
1Hz
HB
HA
H°

B. Conformational Assignment at Low Temperatures

The problem of assigning the two ABX spectra to the appropriate conformations was solved by making use of the data available for a similar molecule, α, α , 2, 4, 6 - pentachlorotoluene (PCT).

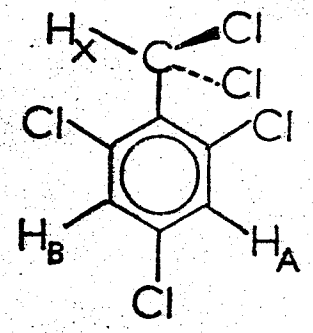

III

The values reported by Fuhr (17) for J_{AX} and J_{BX} are 0.48±0.02Hz and less than 0.1Hz, respectively. The similarity between PCT and 2, 3, 6 - PCT suggests similar stereospecific coupling constants for 2, 3, 6 - PCT. It can be seen from the previous diagrams for 2, 3, 6 - PCT that the "Zig-Zag" pathway between the $H_{X(II)}$ and $H_{B(II)}$ protons of 2, 3, 6 - PCT is essentially the same as the pathway between the H_X and H_A protons of III. It is also clear that the $H_{X(I)}$ and $H_{B(I)}$ protons of 2, 3, 6 - PCT are spatially related in the same way as the H_X and H_B protons in III. Therefore, one may predict with some confidence that $J_{BX(II)} \simeq$ 0.5Hz and $J_{BX(I)} < 0.1$Hz. Schaefer et al have reported similar stereospecific coupling constants for α, α, 2, 6 - tetrachlorotoluene (18).

Knowing these stereospecific coupling constants it is then a simple task to assign the correct ABX spectrum to the corresponding rotamer. It is well known that for systems which have small internal shifts, small long range coupling constants are not observable due to the phenomenon of virtual coupling (3). If the quartet with the internal shift of δ_{AB} = 10.41Hz belongs to conformation II, then the coupling constant of 0.5Hz will be evident in the spectrum. However, if the tightly coupled quartet (δ_{AB} = 2.54Hz) belongs to conformation II, then no splitting due to $J_{B(II)X(II)}$ ≈0.5Hz will be apparent. In the actual spectrum, no splitting due to a coupling constant in the order of 0.5Hz is observed (although the spectrometer is capable of resolving splittings of 0.2Hz quite easily). Therefore, the correct assignment must be the latter. Thus, for conformation II:

$$\delta_{A(II)B(II)} = 2.54\text{Hz}$$

$$J_{B(II)X(II)} = 0.5\text{Hz}$$

and for conformation I:

$$\delta_{A(I)B(I)} = 10.41\text{Hz}$$

$$J_{B(I)X(I)} = 0.1\text{Hz}$$

The computer program, DNMR (15), used to simulate the high resolution spectra in the study of the rate process, vividly illustrates the correctness of the conformational

assignment. The computer was instructed to simulate the low temperature spectra associated with each of the two possible conformational assignments. In figures 7(a) and 7(b), the Calcomp plots of the two possibilities have been reproduced. In figure 7(a) the Calcomp spectrum represents the incorrect assignment (i.e. the AB quartet with δ_{AB} = 10.41Hz belonging to conformation II). In figure 7(b) the Calcomp spectrum represents the correct assignment (i.e. the AB quartet with δ_{AB} = 2.54Hz belonging to conformation II). Above each of the Calcomp plots the spectra are illustrated schematically beside the corresponding conformations. The striking similarity between the Calcomp plot of figure 7(b) and the actual experimental spectrum (cf. figure 1) leaves little doubt about the accuracy of this assignment.

FIGURE 7(a)

Incorrect conformational assignment at low temperatures.

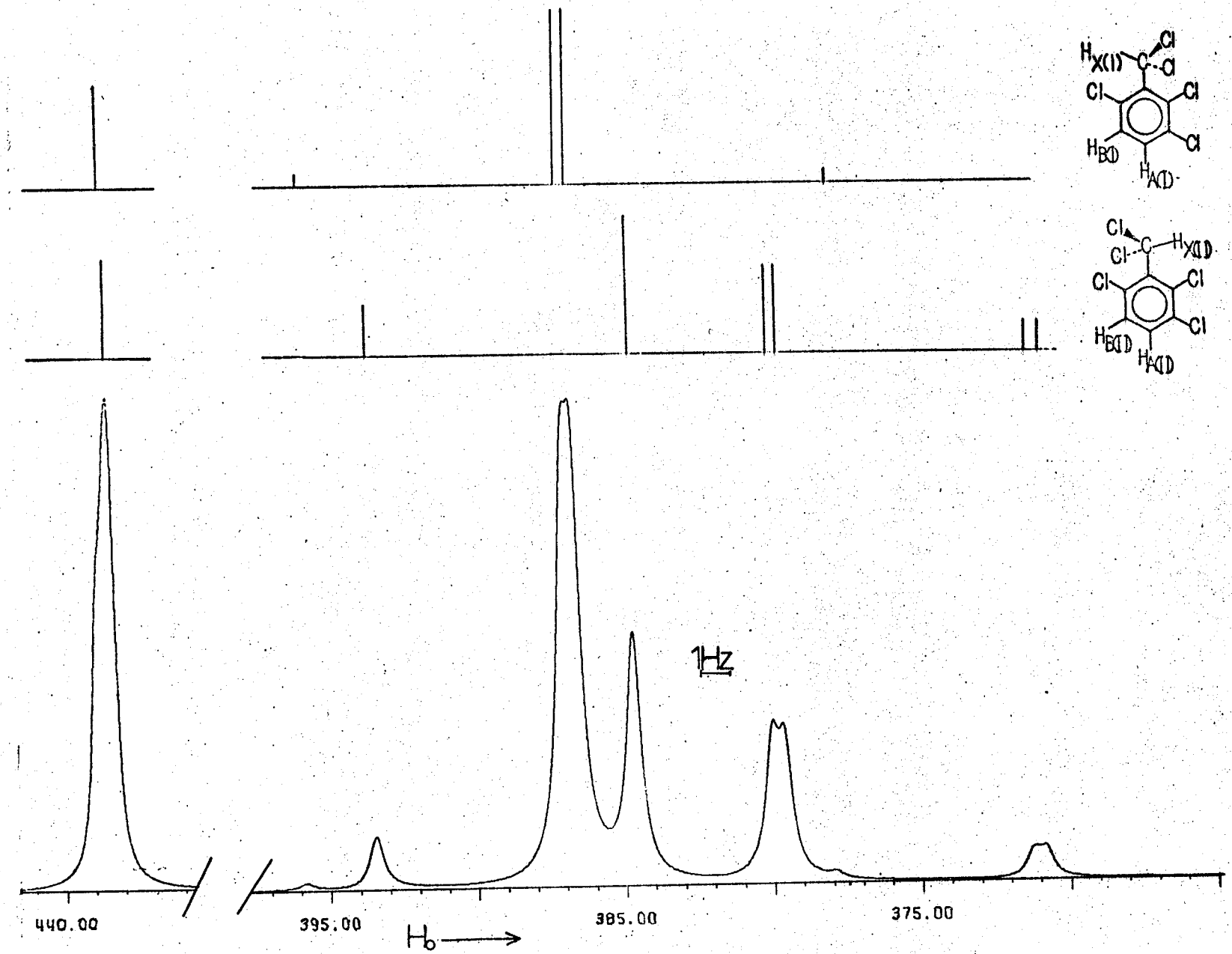

38(a).

FIGURE 7(b)

Correct conformational assignment at low temperatures.

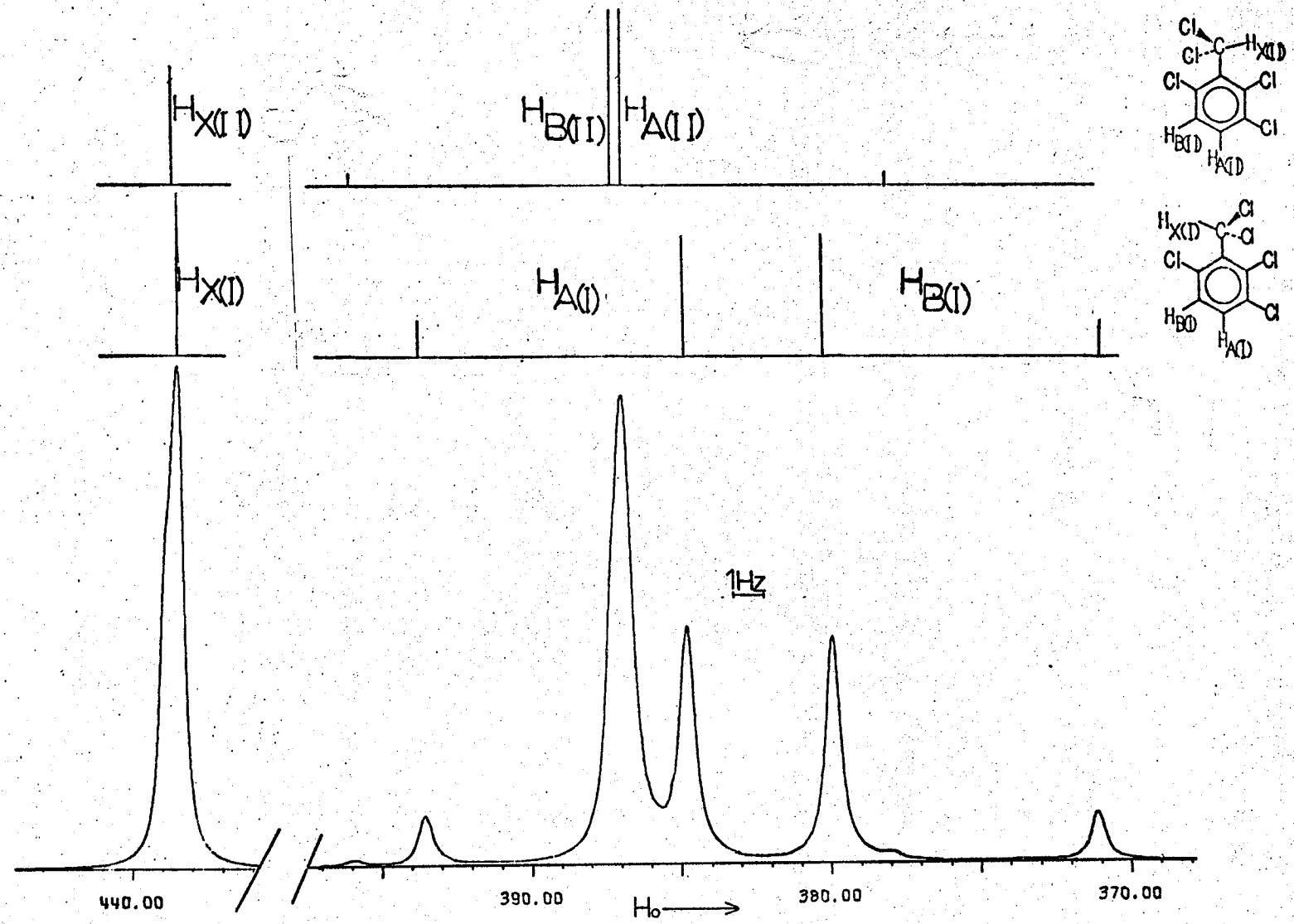

38(b).

C. Proton Assignments

In the preceding section the assignment of the quartets to the correct conformation was discussed. However, nothing has yet been said about how the various peaks within the two quartets were assigned to the correct protons. It is the purpose of this section to explain how this was accomplished.

1. Proton Assignment of High Temperature Spectra

In the high temperature region above the coalescence temperature, the PMR spectrum of 2, 3, 6 - PCT consists of an asymmetrical AB quartet and a sharp methine proton peak. (See figure 6). The two high field peaks of the quartet are somewhat broader than the two low field peaks, presumably because of long range coupling from the methine proton to the H_B proton (17,18). If $J_{B(II)X(II)} = 0.5$ Hz and $J_{B(I)X(I)} < 0.1$Hz, then the peaks due to the H_B proton will be approximately 0.3 Hz broader than those due to the H_A protons in the limiting case when the rotation is very rapid and the coupling constants are averaged.* This reasoning suggests that the H_B proton lies to high field of the H_A proton in the high temperature region. The coupling constants, chemical shifts and line widths of the high temperature region are given in table 1.

* $J_{AX} \simeq 0$. Then in the limit of rapid rotation $\frac{J_{BX(I)} + J_{BX(II)}}{2}$

$\simeq \frac{0.5 + 0.1}{2} \simeq 0.3$ and $\frac{J_{AX(I)} + J_{AX(II)}}{2} \simeq 0.$

TABLE 1

Chemical shifts, coupling constants and line widths of the ring protons at temperatures above the coalescence temperature

					Half Height Linewidths				
Temp(°K)	δ_{AB}(Hz)*	δ_A	δ_B	J_{AB}	Line #1	Line #2	Line #3	Line #4	1/T
323.5	4.88±.25**	400.89±.18	396.01±.01	8.80±.12	0.53±.05	0.68±.05	1.6±.1	1.2±.1	3.091×10^{-3}
333.0	4.99±.18	402.37±.14	397.38±.14	8.79±.19	0.40±.01	0.53±.02	0.93±.01	0.73±.04	3.030×10^{-3}
343.7	5.08±.16	403.88±.11	398.80±.11	8.74±.06	0.36±.01	0.49±.05	0.64±.06	0.58±.03	2.909×10^{-3}
349.2	5.12±.11	404.80±.09	399.68±.09	8.74±.07	0.35±.05	0.42±.03	0.58±.02	0.50±.01	2.864×10^{-3}
361.5	5.21±.11	406.26±.10	401.06±.10	8.72±.08	0.35±.04	0.41±.04	0.54±.03	0.53±.04	2.766×10^{-3}
378.2	5.34±.24	408.24±.17	402.90±.17	8.76±.10	0.33±.09	0.47±.04	0.56±.05	0.45±.04	2.644×10^{-3}

* All chemical shifts, coupling constants and linewidths are reported in Hertz as obtained at 60MHz unless otherwise indicated.

**Errors quoted are the standard deviations.

In the temperature range above coalescence the chemical shift of a particular proton is simply a weighted mean (3) (with respect to populations) of the chemical shifts of the two exchanging protons in the absence of exchange.

That is, at high temperatures *

$$\delta_A = P_{(I)}\delta_{A(I)} + P_{(II)}\delta_{A(II)} \qquad (4\text{-}1)$$

$$\delta_B = P_{(I)}\delta_{B(I)} + P_{(II)}\delta_{B(II)} \qquad (4\text{-}2)$$

where δ_A, δ_B are the high temperature chemical shifts of A and B respectively,

$\delta_{A(I)}$, $\delta_{A(II)}$, $\delta_{B(I)}$, $\delta_{B(II)}$ are the low temperature chemical shifts of A(I), A(II), B(I), B(II) respectively, and

$P_{(I)}$, $P_{(II)}$ are the relative populations ** of conformations I and II normalized to 1.

* These equations are rigorously valid only in an ideal solution where there are no solvent effects. It was found, however, that for a 20 mole % solution of 2, 3, 6 - PCT in toluene - d_8 that all solvent effects were linear with respect to 1/T. Hence, it is a simple task to make the appropriate alterations to equations (4-1) and (4-2). Solvent effects are fully discussed in a later section.

** It is suggested in a later section that the ratio, $P_{(I)}/P_{(II)} = 0.91$, is essentially constant over the temperature range of the rate study.

If a plot of the high temperature chemical shifts δ_A and δ_B versus 1/T is made*, then the weighted mean of $\delta_{A(I)}$ and $\delta_{A(II)}$, and $\delta_{B(I)}$ and $\delta_{B(II)}$ can be deduced at any temperature. Such a plot is shown in figure 8. In figure 9, a straight line plot* of δ_{AB} versus 1/T has been reproduced.

2. Proton Assignment of Low Temperature Spectra.

Consider the spectra of 2, 3, 6 - PCT at temperatures below the coalescence temperature. The relevant data are given in tables II and III. At 254.6°K (figure 1) there are two AB quartets with $\delta_{A(I)B(I)}$ = 10.41Hz and $\delta_{A(II)B(II)}$ = 2.54Hz. There are in fact, four possible assignments of the protons of low temperatures; they are shown in figure 10. Each of these four combinations predict a different weighted average of δ_{AB} as defined by

$$\delta_{AB} = \{P_{(I)}\delta_{A(I)}+P_{(II)}\delta_{A(II)}\} - \{P_{(I)}\delta_{B(I)}+P_{(II)}\delta_{B(II)}\} \quad (4\text{-}3)$$

The four internal chemical shifts (δ_{AB}) predicted by each of the four possible assignments are given in table IV.

* Such a graph inherently takes into account any solvent effects.

FIGURE 8

High temperature chemical shifts versus 1/T.

Data plotted found in table I.

$\delta_A = (-16{,}950 \pm 133)\ 1/T + (453.26 \pm .44)$

correlation coefficient = 0.99969

$\delta_B = (-15{,}760 \pm 130)\ 1/T + (444.75 \pm 0.41)$

correlation coefficient = 0.99969

Legend: δ_A ..... □

δ_B ..... ■

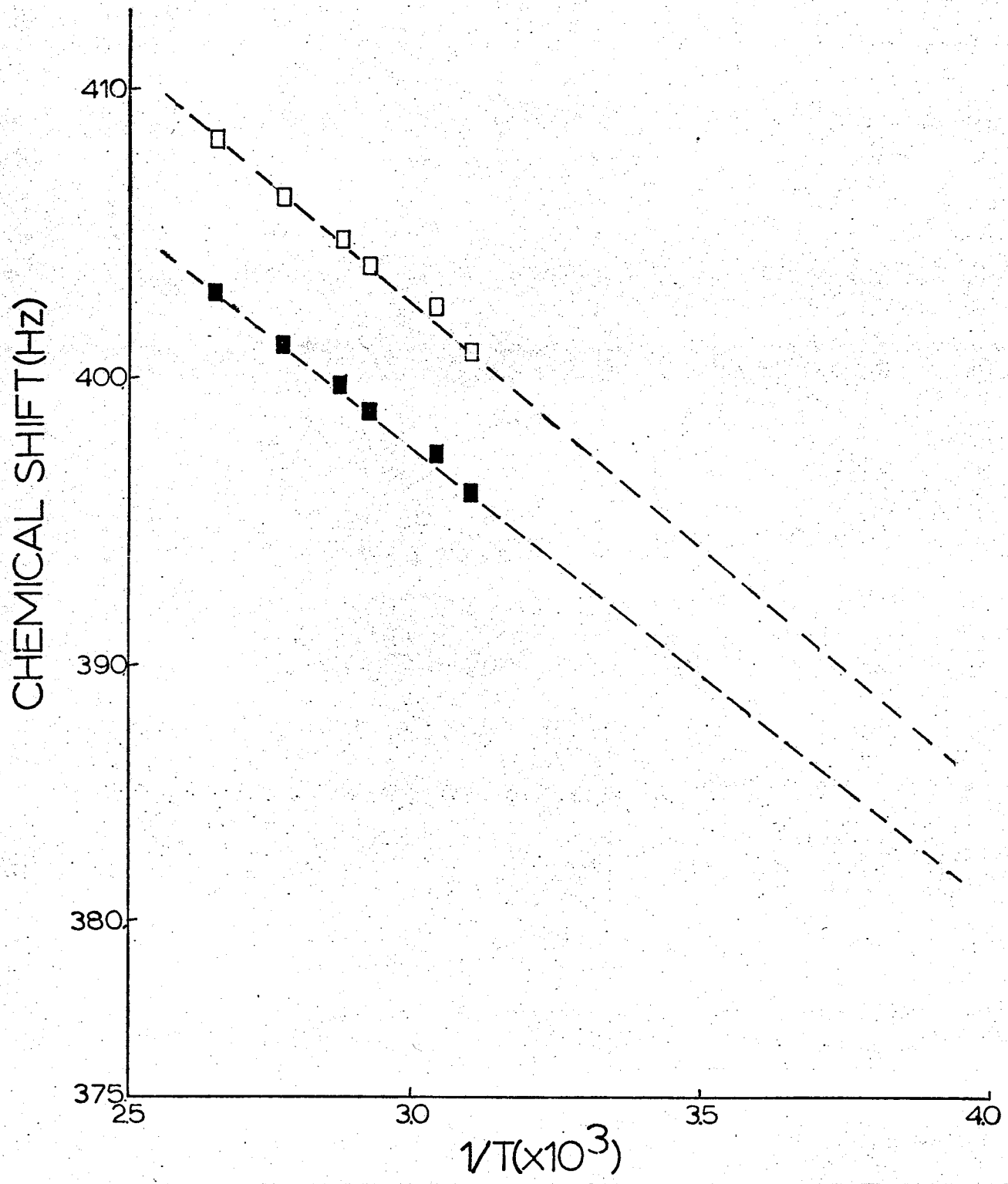
CHEMICAL SHIFT(Hz)
410
400
390
380
375
2.5
3.0
3.5
4.0
1/T(x10-3)

FIGURE 9

A plot of δ_{AB} versus 1/T.

Data plotted found in table I.

$\delta_{AB} = (-955 \pm 41)\ 1/T + (7.86 \pm .12)$

correlation coefficient 0.9945

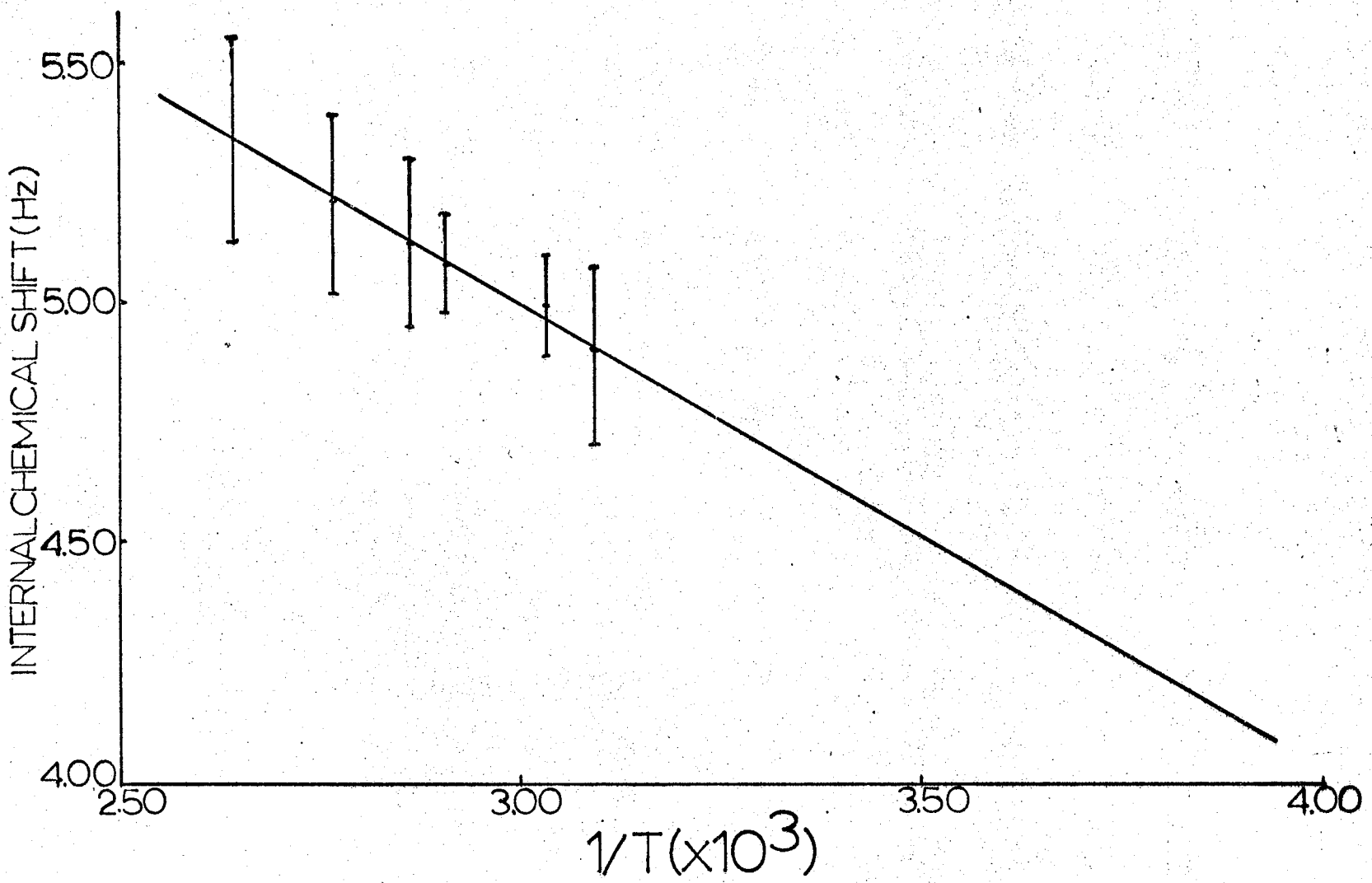
INTERNAL CHEMICAL SHIFT (Hz)
5.50
5.00
4.50
4.00
2.50
3.00
3.50
4.00
1/T (x10³)

TABLE II

Chemical shifts and coupling constants for the protons of conformation I at temperatures below the coalescence temperature.

Temp(°K)	$\delta_{A(I)}$(Hz)*	$\delta_{B(I)}$(Hz)	$\delta_{AB(I)}$	$\delta_{X(I)}$	Center I**	$J_{AB(I)}$(Hz)
254.6	387.54±.09***	377.14±.09	10.41±.12	438.40±0.1	382.34±.03	8.76±.07
258.0	388.45±.09	378.01±.09	10.44±.10	439.03±.02	383.23±.04	8.78±.13
266.7	390.97±.19	380.47±.19	10.51±.23	439.69±.05	385.72±.07	8.74±.16
275.7	392.72±.16	382.15±.16	10.57±.17	440.20±.01	387.43±.07	8.65±.17

*All chemical shifts are reported in Hz at 60MHz unless otherwise indicated.

**The center of the AB quartet belonging to conformation I was obtained by taking the mean of the 4 lines comprising the quartet.

***The errors quoted are the standard deviations.

TABLE III

Chemical shifts and coupling constants for the protons of conformation II at temperatures below the coalescence temperature.

TEMP	$\delta_{A(II)}$*	$\delta_{B(II)}$	$\delta_{AB(II)}$	$\delta_{X(II)}$	CENTER II	$J_{AB(II)}$
254.6	385.7	388.2	2.54	438.75±.1	386.96±.02	8.89±.15
258.0	386.5	389.0	2.54	439.03±.02	387.71±.09	8.89±.15
266.7	388.9	391.4	2.54	439.69±.05	390.14±.14	8.89±.15
275.7	390.5	393.0	2.54	440.20±.01	391.73±.08	8.89±.15

*The chemical shift between the two ring protons of conformation II is too small to permit normal analysis of the AB quartet. The splitting of the two central peaks is not resolved and hence an exact evaluation of $\delta_{AB(II)}$ is not possible from the 60 MHz spectra. The same quartet is, however, adequately resolved in the 100 MHz spectra. Therefore, it is possible to evaluate $\delta_{AB(II)}$ at 100 MHz and consequently to determine that the shift at 60 MHz at 243°K is 2.54Hz. By adding or substracting 2.54/2 to the center of the quartet at 60 MHz, one is able to obtain the proton shifts of $H_{B(II)}$ and $H_{A(II)}$.

The coupling constant $J_{AB(II)}$ was obtained as well from the 100 MHz spectra.

FIGURE 10

The four possible proton assignments at low temperatures.

1. $H_{B(I)}$ — 387.54Hz; $H_{A(I)}$ — 377.14Hz

$H_{B(II)}$ — 388.2Hz; $H_{A(II)}$ — 385.7Hz

2. $H_{A(I)}$ — 387.54; $H_{B(I)}$ — 377.14

$H_{B(II)}$ — 388.2; $H_{A(II)}$ — 385.7

3. $H_{B(I)}$ — 387.54; $H_{A(I)}$ — 377.14

$H_{A(II)}$ — 388.2; $H_{B(II)}$ — 385.7

4. $H_{A(I)}$ — 387.54; $H_{B(I)}$ — 377.14

$H_{A(II)}$ — 388.2; $H_{B(II)}$ — 385.7

TABLE IV

Chemical Shifts of the Four Possible Assignments

Assignment	$P_{(I)}^{*}\delta_{A(I)}+P_{(II)}\delta_{A(II)}$	$P_{(I)}\delta_{B(I)}+P_{(II)}\delta_{B(II)}$	δ_{AB}**
1	381.61	387.88	-6.27
2	386.58	382.91	+3.67
3	382.91	386.58	-3.67
4	387.88	381.61	+6.27

*$P_{(I)}$ and $P_{(II)}$, the populations of conformations I and II respectively, have relative values of 0.48 and 0.52. For a complete discussion of the population difference see Section E.

** A typical error in this value would be ±.3Hz.

Extrapolation of the high temperature data to the low temperature range (see figures 7 and 8) predicts a value for δ_{AB} = +4.10±.28Hz at 254.6°K. Comparison of this value with the values calculated for the four possible proton assignments clearly shows that Assignment #2 is the correct one.

D. Rationalization of the Chemical Shifts

This section concerns the rationalization of the relative shifts of the various protons of 2, 3, 6 - PCT. Although numerical values for the effects contributing to the shifts are not available for the most part, a qualitative explanation of all the chemical shifts is possible. This section has been subdivided into two parts. The first part includes a discussion of the chemical shifts of the ring protons in the absence of the dichloromethyl group (i.e. in 1, 2, 4 - trichlorobenzene), and the second part completes the rationalization with a discussion of the shifts in the presence of the dichloromethyl group.

1. In the Absence of the Dichloromethyl Group

(a) Substituent Effect

Richardson and Schaefer (19) reported an additivity scheme by which the substituent effects on the proton shifts of halogenated benzenes could be predicted. For 1, 2, 4 - trichlorobenzene*, they observed that the proton shift for H_B (i.e. H_5) was 10.86Hz to high field of the shift for H_A (i.e. H_6).

* 3% molar solution in cyclohexane measured at 60MHz.

(b) Solvent Effects

Wasylishen and Schaefer (20) have recently devised an empirical scheme for predicting the effects of solvent on the chemical shifts of polysubstituted benzenes. By using the solvent shift constants* for chlorine in the ortho, meta and para positions (Δ^{Cl}_{o}, Δ^{Cl}_{m} and Δ^{Cl}_{p}) one obtains δ_B and δ_A in an aromatic solvent by simply adding the appropriate constant to the values of δ_B and δ_A recorded in a cyclohexane solution. Relative to their values in cyclohexane the solvent effects predicted for an aromatic solvent are

δ_A = 33.87Hz**

δ_B = 34.62Hz .

It appears from these predictions that the solvent effect on the two protons is almost identical, different only by 0.75Hz. Therefore, both the substituent effects and the solvent effects indicate that in an aromatic solution of 1, 2, 4 - trichlorobenzene, H_B will lie to high field by H_A by approximately (10.86 + 0.75) Hz.

* The solvent shift constants are defined by: Δ = shift in cyclohexane - shift in benzene.

** Hz at 60 MHz.

2. In the Presence of the Dichloromethyl Group

(a) Steric Effects

i) Conformation I

The effect on proton shifts by steric repulsion of two chloro groups in an ortho-disubstituted benzene molecule was measured by Richardson and Schaefer (19). It appears for 2, 3, 6 - PCT that steric interactions between the ring chlorines and the side-chain chlorines influence the proton shifts more strongly than do other effects.

In conformation I, the methyl chlorines sterically repel the ortho chlorine producing a slight buttressing effect on the meta chlorine.

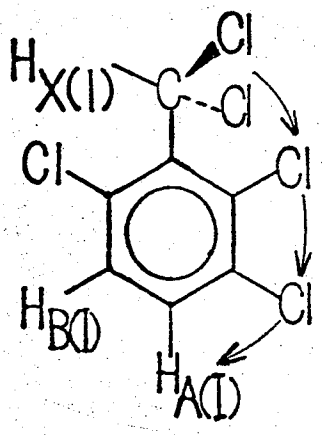

Consequently the H_A proton is slightly deshielded (19) while the H_B proton experiences no net effect because it is far removed from the chlorine-chlorine interactions.

ii) Conformation II

In conformation II, the side-chain chlorines steri-

cally interact with an ortho chlorine forcing it nearer the $H_{B(II)}$ proton.

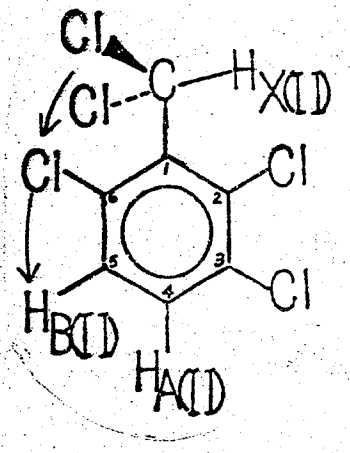

Hence, the $H_{B(II)}$ proton is deshielded as a result of this steric interaction. Consequently, it would be expected on the basis of these steric interactions that the line position of $H_{B(II)}$ would be far downfield from the line position of $H_{B(I)}$. Similar deshielding effects have been reported for α, α, 2, 6 - tetrachlorotoluene (18) and PCT (17).

On the other hand, $H_{A(II)}$ does not experience the small deshielding effect which $H_{A(I)}$ does. The 180° rotation of the dichloromethyl group from conformation I to conformation II results in an increase of the distance between H_A and Cl_3; the slight buttressing effect similar to the one in conformation I, from the methyl chlorines to the H_A proton, is non-existent in conformation II. Therefore, on the basis of steric repulsion, the line position of $H_{A(I)}$ is predictably to lowfield

of $H_{A(II)}$ by a small amount.

One last point should be emphasized; because of the relative proximity of the H_B protons to the dichloromethyl group, their line positions are much more sensitive to rotation of the dichloromethyl group than are the line positions of the H_A protons.

(b) Solvent Effect

i) Conformation I

In general, aromatic solvent molecules prefer to reside as far away as possible from the electron-rich portion of the solute molecule (21). The electron-rich portion of conformation I is located at the dichloromethyl group. Therefore, the solvent molecule is likely to prefer the orientation shown in the diagram below:

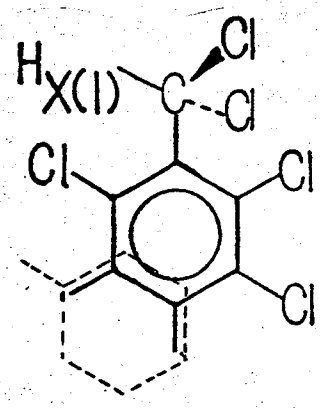

I

Because the H_A and H_B protons are nearly equidistant (6.0Å and 5.6Å respectively*) from the two methyl chlorines, they experience approximately the same solvent shift.

ii) Conformation II

Again, the toluene-d_8 molecule prefers to sit as far away as possible from the two methyl chlorines. However in conformation II the H_A and H_B protons are not equidistant (6.0Å and 4.9Å respectively*) from the two methyl chlorines. Accordingly, the solvent molecule is probably shifted to a position slightly nearer the H_A proton than the H_B proton.

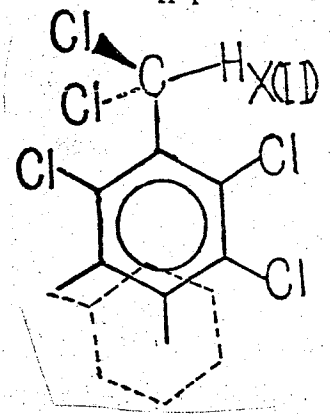

II

Hence one predicts a negligible difference between the effect of the solvent on $H_{A(I)}$ and $H_{A(II)}$, but a downfield shift on $H_{B(II)}$ relative to $H_{B(I)}$.

(c) Dipole Moments

The dichloromethyl group has a dipole moment associated with it. As the dichloromethyl group rotates from conformation

*Based on a scale diagram.

I to conformation II, the direction of the dipole moment changes accordingly. Because the H_A proton is para to the dichloromethyl group, it experiences the same electric field from this dipole in the two conformations. However, the H_B proton in the meta position experiences a different electric field in the two conformations. Nevertheless, considering the relatively large distance between the dichloromethyl group and the ring protons (electric field from the dipole moment decreases as $\frac{1}{r^3}$), it is probably safe to assume that the dipole moment effect on the proton shifts is relatively small.

(d) Summary

Intramolecular steric effects and also solvent effects predict that the $H_{B(II)}$ proton will be shifted downfield from the $H_{B(I)}$ proton. The solvent effect causes little difference between the line positions of $H_{A(I)}$ and $H_{A(II)}$, but the steric effects force $H_{A(II)}$ to be slightly upfield from $H_{A(I)}$. These predictions are in accord with the assignment of the spectra given in Section C.

Finally, the methine protons which lie in the plane of the ring experience the magnetic anisotropy of the ring and hence are strongly deshielded. Furthermore, the interaction of the methine protons with the ortho chlorines seems to be significant. The slight buttressing effect between the

the ortho and meta chlorines apparently makes the interaction between $H_{X(II)}$ and the ortho chlorine larger than the interaction between $H_{X(I)}$ and the ortho chlorine. This would explain why $H_{X(II)}$ is slightly to low field of $H_{X(I)}$. (See Section E)

E. Relative Populations of the Two Conformation

1. Low Temperature Populations

At low temperatures, the two peaks belonging to the methine protons of the two conformations are sufficiently separated to allow an accurate estimation of their relative intensities. Although crystallization of the 2, 3, 6 - PCT at low temperatures restricts the temperature range in which such a determination can be conducted, the results consistently indicate that the low field peak is more intense than the high field peak. A similar estimation of the relative intensities of the two AB quartets was also made. However, because of the large degree of overlap of the two quartets, the results of this investigation are subject to greater random errors. The correlation between the two methine proton peaks and their corresponding quartets is quite evident from table V and table VI; namely, that the high field methine peak originates from conformation I and the low field methine peak originates from conformation II.

Although the estimation of the relative intensities of the methine peaks is restricted to a 10^{o} temperature range, the value of the ratio is essentially constant over this range. Knowing the value for the population ratio allows the calculation of the difference in free energy (ΔG^{o}) between the two

TABLE V

Relative Intensities of the $H_{X(I)}$ and $H_{X(II)}$ peaks in the in the low temperature region.

Temperature	Ratio:* $H_{X(I)}/H_{X(II)}$
233.0°K	.91±.06**
236.5°K	.92±.06
240.5°K	.92±.06
243.0°K	.88±.05***

*The ratios given here were determined by weighing.
**The errors quoted are the standard deviations.
***This value was obtained from 100 MHz spectra.

TABLE VI

Relative intensities of the AB(I) quartet to the AB(II) quartet in the low temperature region.

Temperature	Ratio: AB(I)/AB(II)
243.0°K	0.91±.06*
254.6°K	0.92±.06

* From 100 MHz spectra, the intensity data from the 100 MHz spectra are believed to be more reliable than the 60MHz data because there is a lesser degree of peak overlap.

rotamers at these low temperatures. At 243°K,

$$P_I/P_{II} = \exp\ (-\Delta G^o)/RT$$

where $P_I/P_{II} = 0.91 \pm 0.05$.

Therefore, $\Delta G^o = 50 \pm 20$ cal/mole. Hence at 243°K, conformation II is 50 cal/mole more stable than conformation I.

2. High Temperature Populations

a) The Assumption

The validity of extrapolating the low temperature populations is dubious because it is not known how ΔG^o varies with temperature. Moreover, except for the 10°K range at low temperatures, there was no method available to measure ΔG^o directly. Hence, we make the assumption that the difference in free energy ΔG^o between the two conformations is constant over the temperature range in which the rate study is conducted (254.6°K to 378.2°K). Such an assumption predicts a negligible difference in populations at the two extreme temperatures of the rate study. (At 254.6°, $P_I/P_{II} = 0.91$; at 378.2°, $P_I/P_{II} = 0.93$). This small difference is well within experimental error, and therefore the value 0.91 was used throughout.

b) The Justification

This section discusses the asumption that ΔG^o is independent of temperature.

The difference in free energy is related to the difference in enthalpy ΔH^o and the difference in entropy ΔS^o by the equation,

$$\Delta G^o = \Delta H^o - T\Delta S^o . \qquad (4\text{-}5)$$

It is quite evident that ΔG^o is independent of temperature only if ΔH^o is independent of temperature and ΔS^o is zero. Each of these conditions is now considered.

Govil and Bernstein (22,23) suggest a method for calculating the difference in entropy between two rotamers in solution. In general, the difference between the entropies of two rotamers can be expressed as the sum of contributions from the translational (ΔS_t), vibrational (ΔS_v), and rotational (ΔS_r) motions,

i.e. $$\Delta S^o = \Delta S_t + \Delta S_v + \Delta S_r . \qquad (4\text{-}6)$$

Because the mass of the two rotamers is the same, the contribution from the translational motion is zero. As well, the low-lying vibrational frequencies of the two conformations are likely to be very nearly equal and therefore $\Delta S_v \simeq 0$. Hence, it is the rotational motion which generally makes the greatest contribution to ΔS^o. ΔS_r can be calculated directly from the relationship

$$\Delta S_r = \tfrac{1}{2} \ln \{I_{X(I)}\ I_{Y(I)}\ I_{Z(I)} \,/\, I_{X(II)}\ I_{Y(II)}\ I_{Z(II)}\} \qquad (4\text{-}7)$$

where I_X, I_Y, I_Z are the principal moments of inertia. The

products $I_{X(I)}\ I_{Y(I)}\ I_{Z(I)}$ and $I_{X(II)}\ I_{Y(II)}\ I_{Z(II)}$ are evaluated by drawing a scale diagram of the two conformations and using the method outlined by Davidson (24). It is found, however, that the two products are very nearly identical*. Therefore, the value for ΔS_r calculated from the above equation is effectively zero and hence each of the three contributing terms is zero.

Discussions of the temperature dependence of the enthalpy differences between rotational isomers in liquids have been given elsewhere (3,22,26,41). In most rate studies involving unequally populated conformations, ΔH^o is assumed to be constant (22,23,24). Since $\Delta S^o \simeq 0$, equation (4-5) then implies that ΔG^o and ΔH^o are equal. The continuity which the high temperature chemical shifts display with the weighted average of the low temperature shifts (see section C) is consistent with the assumption that $\Delta G^o (\Delta H^o)$ is temperature independent.

* $I_{X(I)}\ I_{Y(I)}\ I_{Z(I)} = 4.010 \times 10^{17}\ (\text{amu})^2\ (\text{Å})^6$

$I_{X(II)}\ I_{Y(II)}\ I_{X(II)} = 4.015 \times 10^{17}\ (\text{amu})^2\ (\text{Å})^6$

F. The Rate Process

1. Determination of the Rate Constants

a). Computer Program DNMR

Rate constants for the rotation of the dichloromethyl group were obtained by comparing the line-shapes of the experimental spectra with those generated by the computer program DNMR (Dynamic Nuclear Magnetic Resonance). A complete description of the program and the theory on which it is based has been given elsewhere (15,27). Briefly, DNMR is a general line-shape computer program designed for the computation of complex exchange-broadened spectra. Its algorithm is based on a complete quantum mechanical theory of exchange effects on high resolution NMR line-shapes. DNMR generates and plots complex exchange-broadened NMR spectra from input data which include chemical shifts, coupling constants, relaxation times, rate constants, populations and certain scaling parameters.

b). Effective Transverse Relaxation Time

Many alternative methods for selecting an effective transverse time have been suggested in the literature (28-30). Barber (16)and Fuhr (17)obtained their values from a consideration of the half-height linewidth of an impurity peak. Peeling (31) determined the effective transverse relaxation time from the half-height linewidths of his sample in the

region of the slow exchange. For practical reasons we chose to calculate the effective transverse relaxation time for all the protons in 2, 3, 6 - PCT from the half-height linewidth of the peak belonging to the H_A proton at the highest temperature recorded. At this high temperature the linewidth is independent of the exchange process and is determined only by the transverse relaxation mechanism and the resolution of the magnet. The effective transverse relaxation time T_2' is related to the half-height linewidth $\Delta\delta_{\frac{1}{2}}$ by the equation (5):

$$\Delta\delta_{\frac{1}{2}} = \frac{1}{\pi T_2'} \quad . \qquad (4\text{-}8)$$

Hence, for a value of $\Delta\delta_{\frac{1}{2}}$ = .40 Hz,

T_2' = 0.80 seconds.

However, none of the methods outlined above including our own is infallible, and therefore, an inescapable error is introduced into the rate study. This will be further discussed in the section on errors.

c). Solvent Effects

In a previous section it was described how an extrapolation of the high temperature shifts shows continuity with only one of four possible proton assignments at low temperatures. This temperature dependent behaviour of the proton shifts is typical of aromatic solvents like toluene-d_8.

Discussion of this aromatic solvent induced shift (ASIS) is available in several sources (17,32,33).

For a rigorous evaluation of the rate constants, these solvent effects should be taken into account. For a solution of 2, 3, 6 - PCT in toluene - d_8 there are two basic types of temperature dependent solvent effects which were considered. The first one involves determining how the average line position of A(I) and A(II) and the average line position of B(I) and B(II) varies with temperature. The second one involves determing how the separation between A(I) and A(II) and between B(I) and B(II) varies with temperature.

The first problem was solved by a treatment of the high temperature data. The best correlation coefficient was obtained by assuming an inverse relationship* between the chemical shift and temperature. It then becomes a simple matter to calculate the average line positions of the two A protons and the two B protons in the temperature range where the spectra are broadened by exchange. The results of these calculations are given in table VII. The plot of the high temperature chemical shifts of the A and B protons is shown in figure 11.

* It is recalled that in the section discussing the low temperature proton assignments a similar relationship was assumed.

TABLE VII

The calculated ASIS for the average line position of A(I) and A(II) (i.e. δ_A) and the average line position of B(I) and B(II)(i.e. δ_B)

Temperature (°K)	δ_A (Hz)	δ_B (Hz)
378.2	408.24*	402.90*
361.5	406.26*	401.06*
349.2	404.80*	399.68*
343.7	403.88*	398.80*
333.0	402.37*	397.38*
323.5	400.89*	396.01*
323.5	400.87†	396.02†
320.1	400.31†	395.51†
315.5	399.54†	394.79†
309.3	398.46†	393.79†
306.3	397.92†	393.28†
304.5	397.60†	392.99†
301.0	396.95†	392.38†
298.0	396.38†	391.86†
291.0	395.02†	390.58†
289.8	394.77†	390.36†
286.3	394.06†	389.70†
284.5	393.69†	389.34†
281.7	393.09†	388.79†
275.7	391.85†	387.59†

*The values for δ_A and δ_B in the temperature range 323.5 to 378.2°K were measured directly from the experimental spectra.

†Calculated from a plot of δ_A and δ_B Vs. 1/T using the data from the temperature range 323.5°K to 378.2°K. (See figure 11).

The low temperature shift data were used to determine how the separation between A(I) and A(II) and B(I) and B(II) varies with temperature. It was found that this type of solvent shift was small and that it affects the value for the rate constants almost negligibly. Nevertheless, a small correction was made for the separation between B(I) and B(II) in the rate study. The relevant data are given in table VIII, and a plot of $\delta_{B(I)}$, $\delta_{B(II)}$, $\delta_{A(II)}$, $\delta_{A(I)}$ versus 1/T is given in figure 11.

By making use of the data in tables VII and VIII and figure 11, one may calculate what $\delta_{A(I)}$, $\delta_{A(II)}$, $\delta_{B(I)}$, $\delta_{B(II)}$ would be at any temperature in the absence of exchange. These calculated values are recorded in table IX.

Because the separation between A(I) and A(II) is so small (about 2Hz), the corresponding peaks are relatively insensitive to changes in the rate constants and hence it is unnecessary to make corrections for the solvent shifts $\delta_{A(I)A(II)}$. The separation between the two B protons is much greater, however, and the peaks belonging to the B protons demonstrate dramatic changes as the rate constant is varied. For this reason we directed the greater part of our attention and effort to fitting the peaks belonging to the B protons.

TABLE VIII

Calculated ASIS for the separation between B(I) and B(II) (i.e. $\delta_{B(I)B(II)}$) and A(I) and A(II) (i.e. $\delta_{A(I)A(II)}$).

Temperature	$1/Tx10^{-3}$	$\delta_{B(I)B(II)}$*	$\delta_{A(I)A(II)}$†
254.6	3.928	11.06	1.85
258.0	3.876	11.00	1.95
266.7	3.750	10.93	2.07
275.7	3.627	10.85	2.22
281.7	3.551	10.79	-
284.5	3.515	10.77	-
286.3	3.495	10.76	-
289.8	3.451	10.73	-
291.0	3.436	10.72	-
298.0	3.356	10.67	-
301.0	3.322	10.65	-
304.5	3.284	10.61	-
306.3	3.265	10.60	-
309.3	3.233	10.58	-
315.5	3.170	10.54	-
320.1	3.124	10.51	-
323.5	3.091	10.49	-
333.0	3.003	10.44	-
343.7	2.909	10.40	-
349.2	2.864	10.36	-
361.5	2.766	10.31	-
378.2	2.644	10.20	-

* Values reported for the temperature range 254.6 to 275.7°K were measured from the experimental spectra. The values for the temperature range 281.7 to 378.2 were calculated from the least squares treatment of $\delta_{B(I)B(II)}$ vs. 1/T.

$\delta_{B(I)B(II)} = (667\pm39)\ 1/T + (8.43\pm.13)$
correlation coefficient = .9933

† Because of the relatively small values for $\delta_{A(I)A(II)}$ no correction was made for the ASIS on $\delta_{A(I)A(II)}$.

FIGURE 11

Chemical shifts of the ring protons versus 1/T.

Data plotted found in tables VII and IX.

$\delta_A = (-16{,}950 \pm 133)\ 1/T + (453.26 \pm 0.44)$

correlation coefficient = 0.99969

$\delta_B = (-15{,}760 \pm 130)\ 1/T + (444.75 \pm 0.41)$

correlation coefficient = 0.99969

Legend:

δ_B at high temperatures ■

δ_A at high temperatures □

$\delta_{B(II)}$ at low temperatures ▲

$\delta_{B(I)}$ at low temperatures ●

$\delta_{A(II)}$ at low temperatures △

$\delta_{A(I)}$ at low temperatures ○

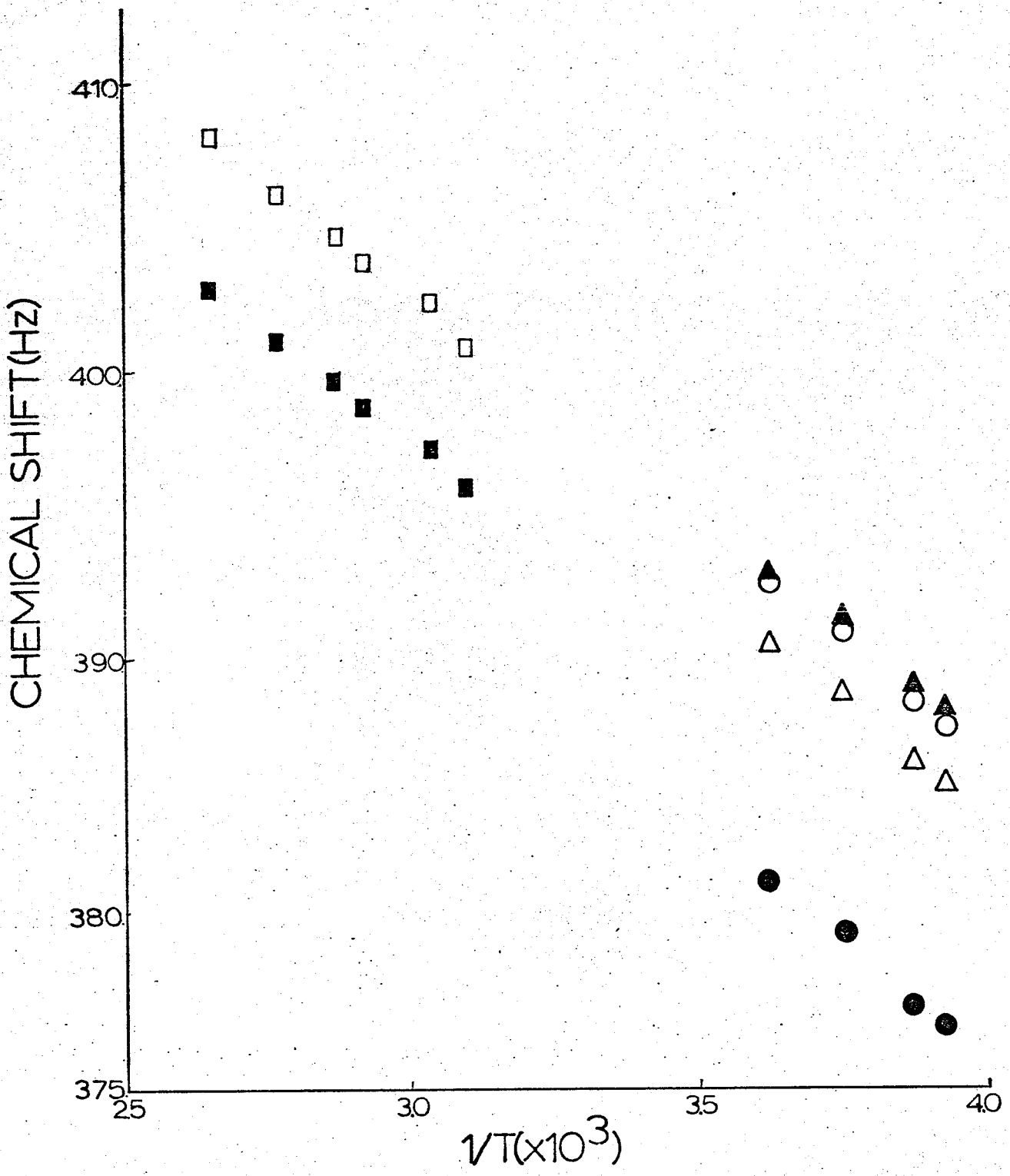
CHEMICAL SHIFT(Hz)
410
400
390
380
375
2.5
3.0
3.5
4.0
1/T(x10^3)

TABLE IX

Calculated values for the chemical shifts of the ring protons of 2,3,6-PCT.

Temp (°K)	$\delta_{A(I)}$	$\delta_{B(I)}$	$\delta_{A(II)}$	$\delta_{B(II)}$
254.6*	387.54	377.14	385.7	388.2
258.0	388.45	378.01	386.5	389.0
266.7	390.97	380.47	388.9	391.4
275.7	392.72	382.15	390.5	393.0
281.7	394.00	383.39	392.20	394.19
284.5	394.59	383.96	392.79	394.72
286.3	394.96	384.32	393.16	395.08
289.8	395.67	385.00	393.87	395.72
291.0	395.92	385.22	394.12	395.94
298.0	397.28	386.53	395.48	397.19
301.0	397.85	387.06	395.05	397.70
304.5	398.50	387.68	396.70	398.30
306.3	398.82	387.98	397.02	398.58
309.3	399.36	388.50	397.56	399.08
315.5	400.44	389.52	398.64	400.06
320.1	401.21	390.26	399.41	400.76
323.5	401.77	390.78	399.97	401.26
333.0	403.47	392.16	401.27	403.60
343.7	404.80	393.60	402.98	404.00
349.2	405.70	394.50	403.90	404.86
361.5	407.16	395.91	405.36	406.21
378.2	409.35	397.97	407.55	408.17

* The values reported for the temperature range 254.6 to 275.7 inclusive were measured directly from the experimental spectra. The remaining values for temperatures 281.7 to 378.2 were calculated from the data given in tables VII and VIII.

By varying the rate constants and making the appropriate corrections for the solvent shifts, the experimental spectra were fitted to the Calcomp plots generated by the computer. Representative experimental and calculated spectra at various temperatures are shown in figures 12 to 17. The rate constants† corresponding to the various temperatures are found in table X.

2. Calculation of the Activation Parameters

Two methods were used to calculate the activation parameters of the rotation. From Eyring's transition-state theory (the absolute reaction rate theory) one obtains the equation:

$$\log \left(\frac{k}{T}\right) = \frac{-\Delta H_I^{\neq}}{2.303R} \left(\frac{1}{T}\right) + \log \frac{\kappa k_b}{h} + \frac{\Delta S_I^{\neq}}{2.303R} \qquad (4\text{-}9)$$

Hence a plot of $\log \left(\frac{k}{T}\right)$ versus 1/T (see table X) gives a straight line whose slope and intercept* are proportional to $\Delta H_I^{\neq}$ and $\Delta S_I^{\neq}$ respectively. Such a plot is reproduced in figure 18. Knowing $\Delta H_I^{\neq}$ and $\Delta S_I^{\neq}$, one may calculate $\Delta G_I^{\neq}$, the free energy activation, from the equation:

$$\Delta G_I^{\neq} = \Delta H_I^{\neq} - T\Delta S_I^{\neq}. \qquad (4\text{-}10)$$

The results of these calculations are recorded in table XI.

† These rate constants correspond to the rate process from conformation I to conformation II.

* κ was assumed to be ½ since the potential energy diagram is essentially symmetrical about the transition state (34,35).

TABLE X

Rate constants at various temperatures

T(°K)	$1/Tx10^3$	k†	k/T	log(k/T)	log k
254.6*	3.928	0.35	-	-	-
258.0*	3.876	0.80	-	-	-
266.7*	3.750	1.5±.25	0.0056	-2.250	0.176
275.7	3.627	2.75±.25	0.0099	-2.001	0.439
281.7	3.549	4.25±.25	0.0151	-1.820	0.628
284.5	3.515	5.25±.25	0.0185	-1.734	0.720
286.3	3.493	6.0±.25	0.0209	-1.679	0.778
289.8	3.451	8.75±.5	0.0302	-1.520	0.942
291.0	3.436	8.75±.5	0.0301	-1.522	0.942
298.8	3.356	16.0±1.5	0.0537	-1.270	1.204
301.0	3.322	24.0±2.5	0.0797	-1.098	1.380
304.5	3.284	31.0±3	0.1018	-0.992	1.491
306.3	3.265	32.5±3	0.1061	-0.974	1.512
309.3	3.233	36.5±4	0.1180	-0.928	1.562
315.5	3.170	56.0±5	0.1775	-0.751	1.748
320.1	3.124	85.0±10	0.2655	-0.576	1.929
323.5	3.091	110±15	0.3400	-0.468	2.041
333.0	3.003	350±50	1.051	+0.022	2.54
343.7*	-	-	-	-	-
349.2*	-	-	-	-	-
361.5*	-	-	-	-	-
378.2*	-	-	-	-	-

† These rate constants were evaluated using the shift data in table IX, $T_2 = 0.80$ sec^{-1}, $J_{AB(I)} = J_{AB(II)} = 8.75$ Hz, $J_{AX(I)} = = J_{AX(II)} = -0.1$Hz, $J_{BX(II)} = 0.5$ Hz and $J_{BX(I)} = 0.1$Hz.

* Values for these temperatures were found to have large error limits and were not included in the evaluation of the activation parameters.

FIGURE 12

Experimental and calculated PMR spectra of a 20 mole % solution of 2, 3, 6 - PCT in toluene-d_8 at 254.6°K

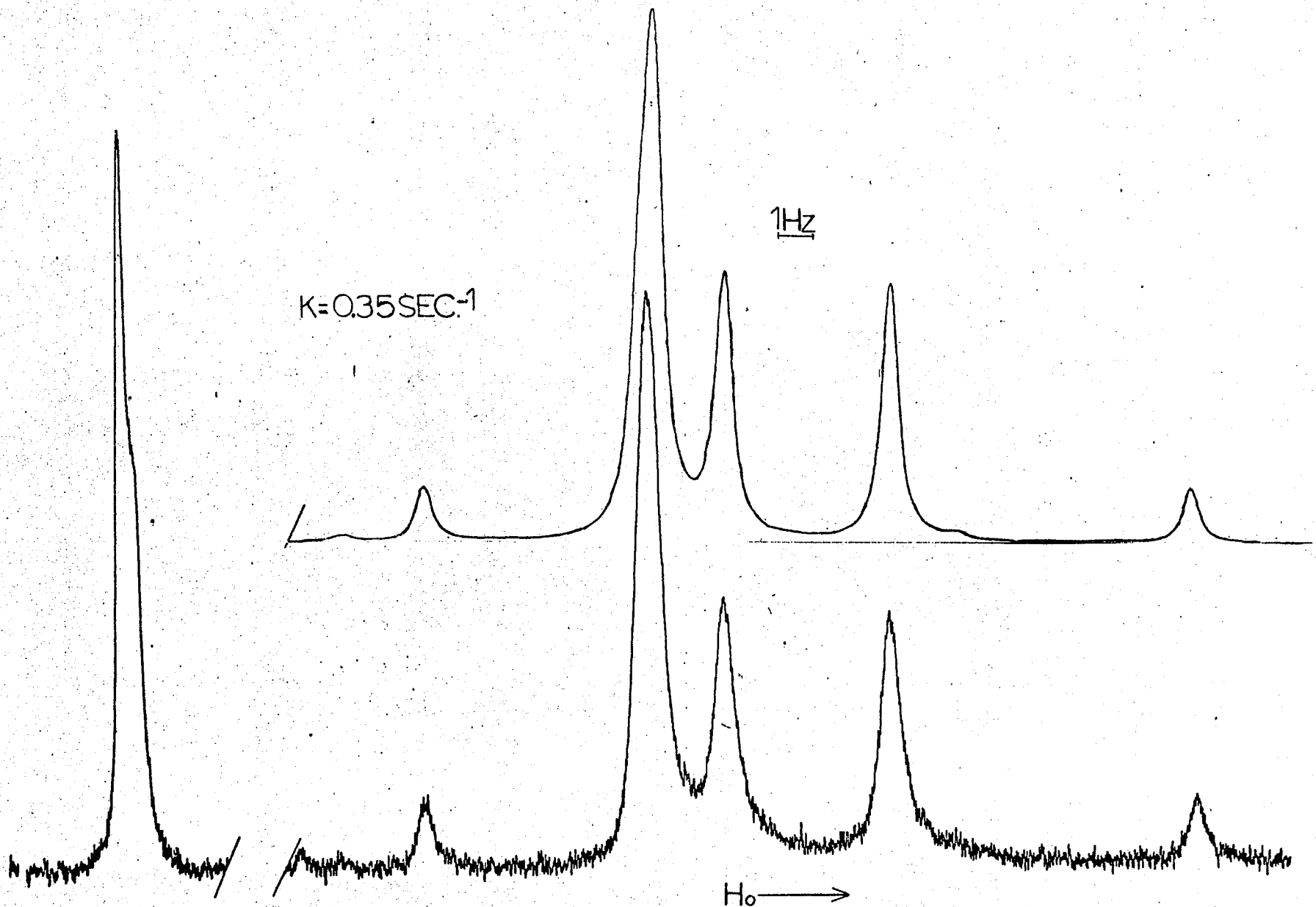
1Hz
K=0.35SEC.-1
Ho

FIGURE 13

Experimental and calculated PMR spectra of a 20 mole % solution of 2, 3, 6 - PCT in toluene-d_8 at 275.7°K

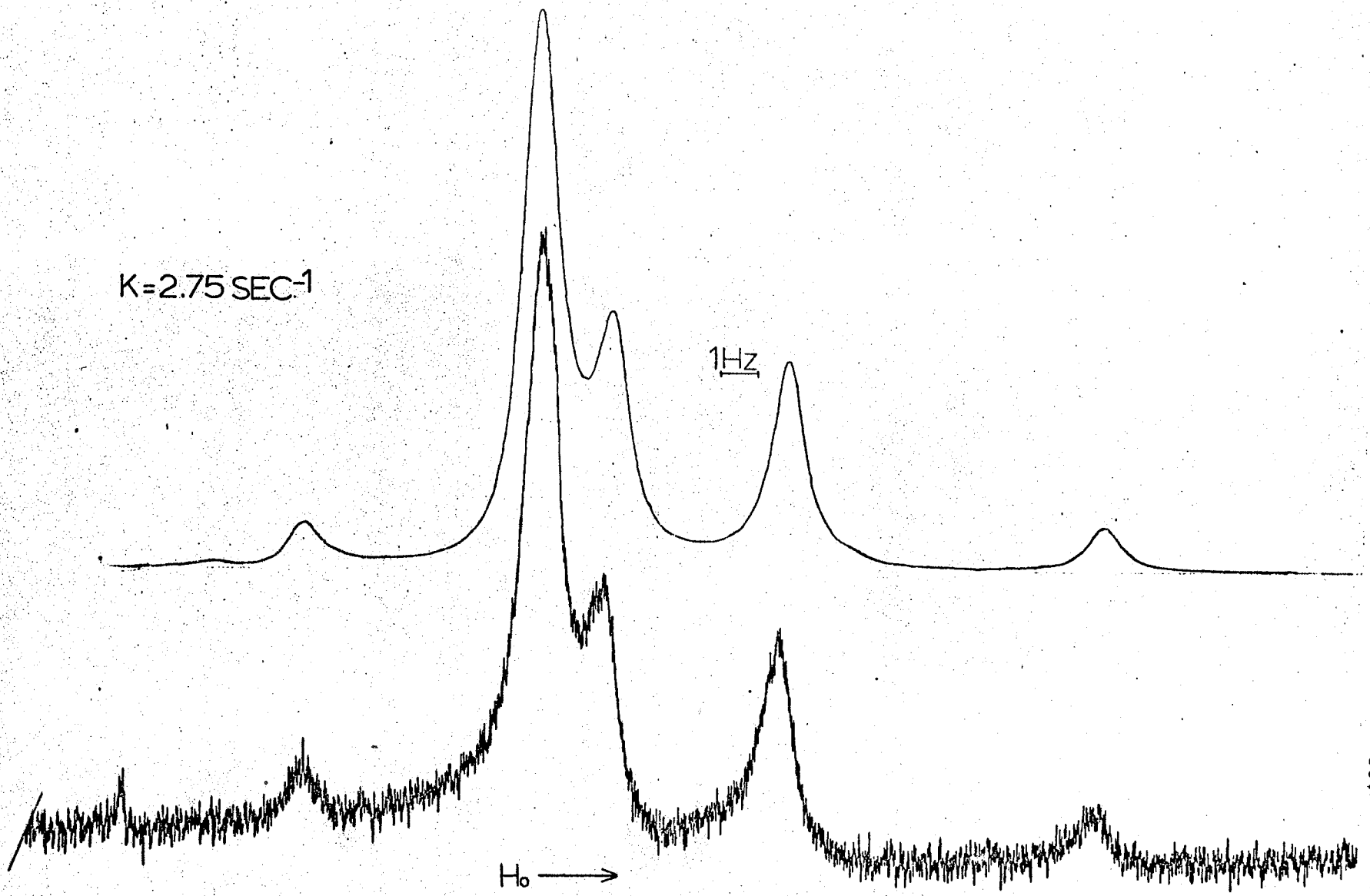

80.

FIGURE 14

Experimental and calculated PMR spectra of a 20 mole % solution of 2, 3, 6 - PCT in toluene-d_8 286.3°K

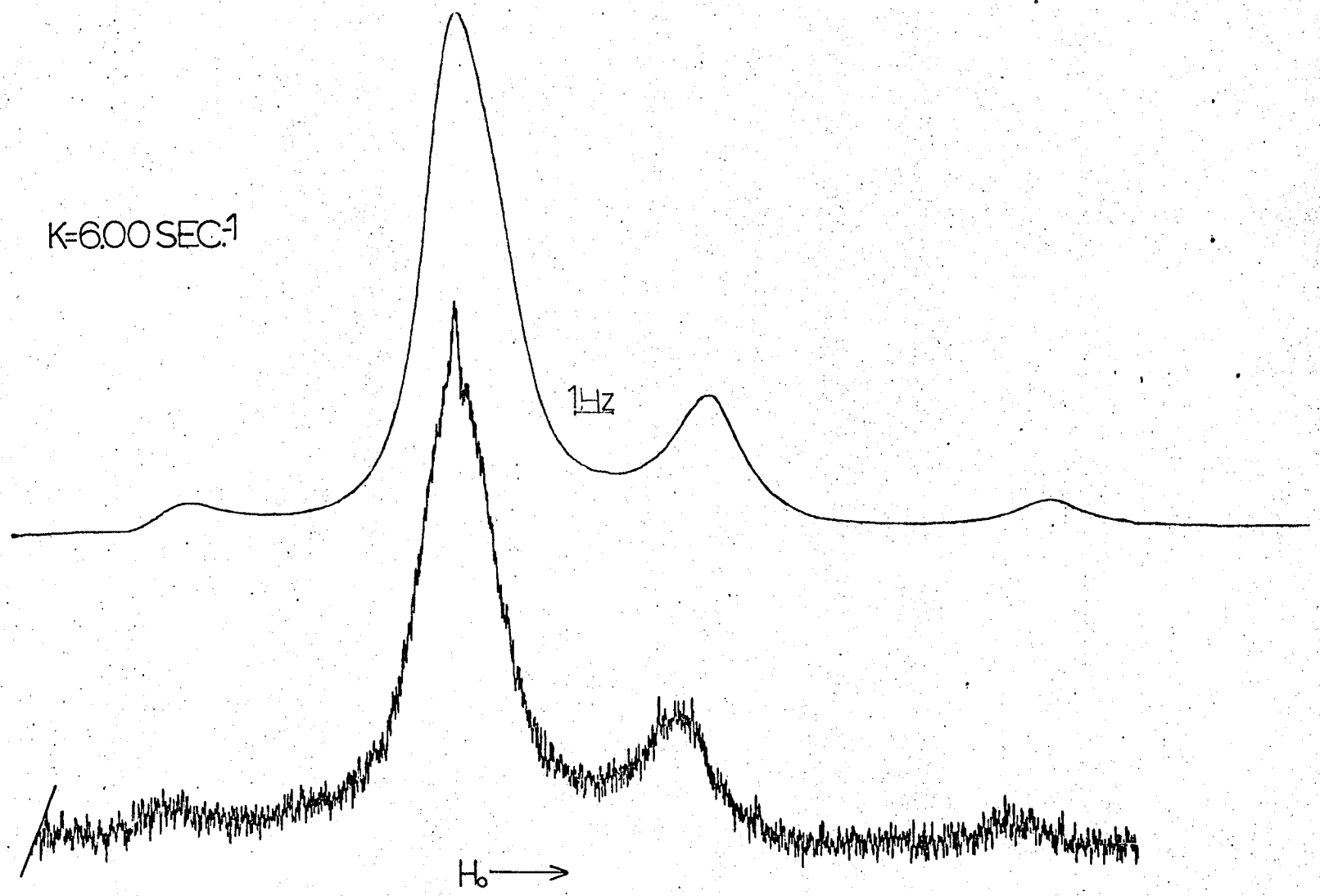
K=6.00 SEC.-1
1 Hz
H₀

FIGURE 15

Experimental and calculated PMR spectra of a 20 mole % solution of 2, 3, 6 - PCT in toluene-d_8 at 298.8°K

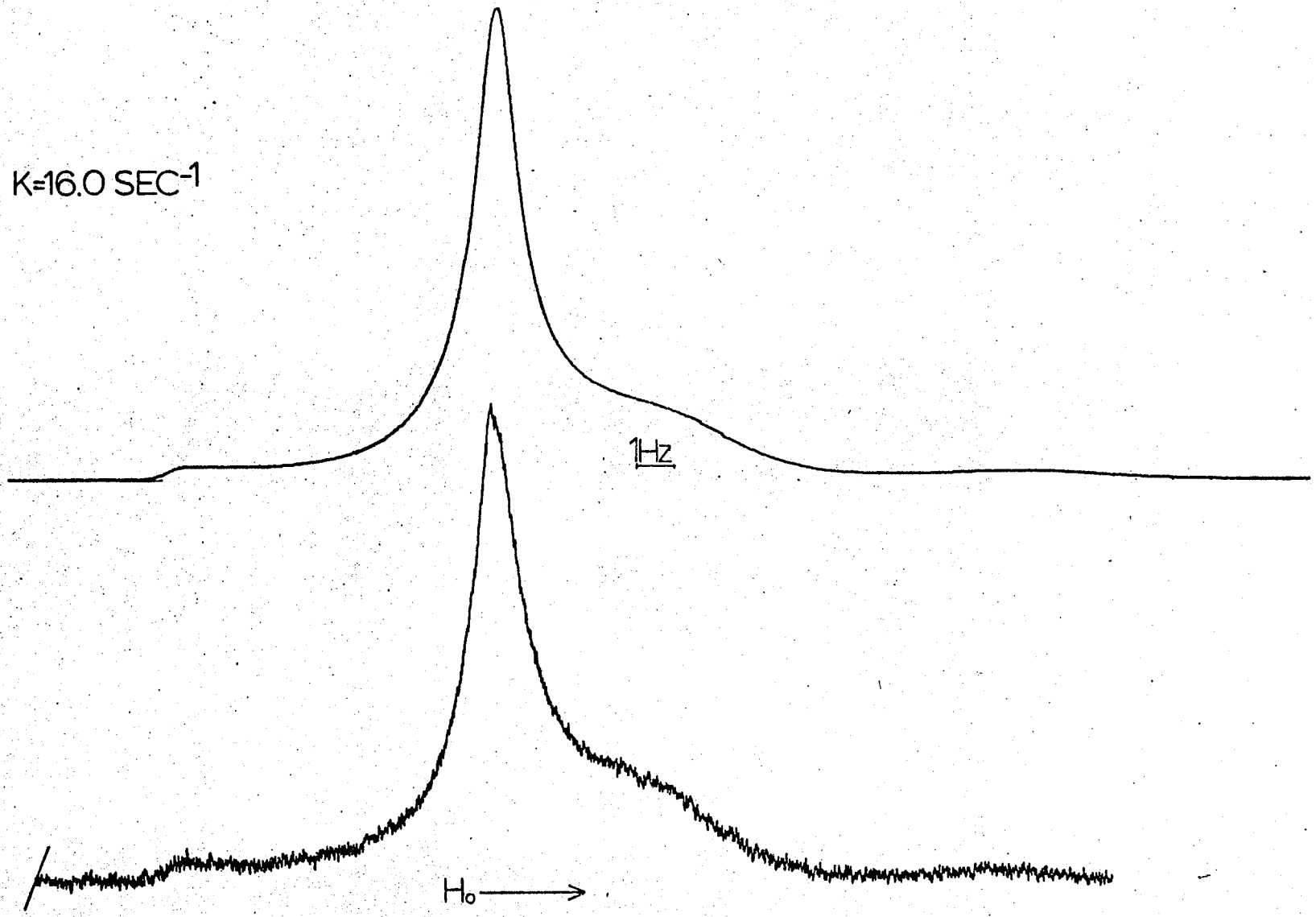
K=16.0 SEC-1
1Hz
Ho

FIGURE 16

Experimental and calculated PMR spectra of a 20 mole % solution of 2, 3, 6 - PCT in toluene-d_8 at 320.1°K

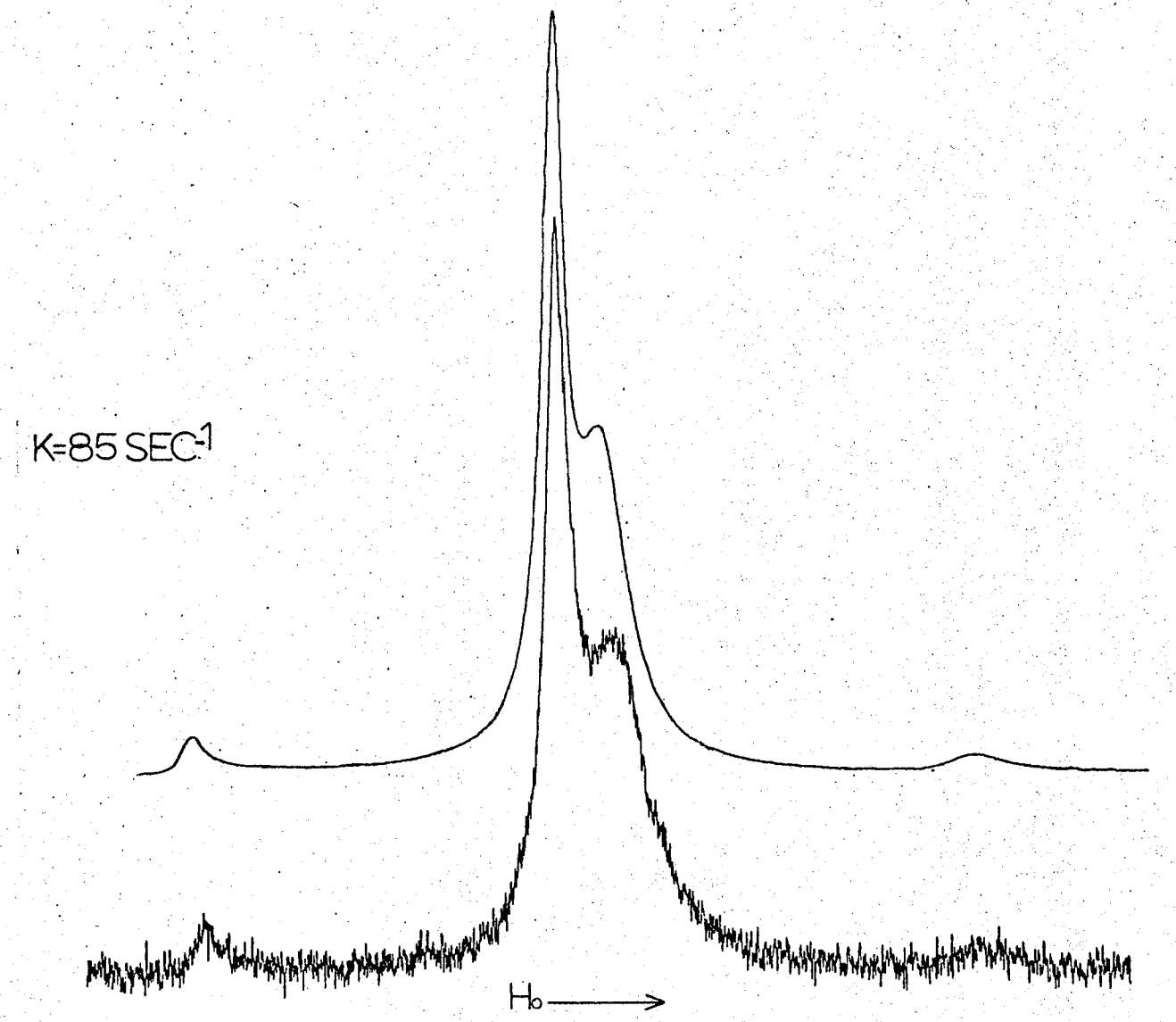
K=85 SEC-1
H₀

FIGURE 17

Experimental and calculated PMR spectra of a 20 mole % solution of 2, 3, 6 - PCT in toluene-d_8 at 378.2°K

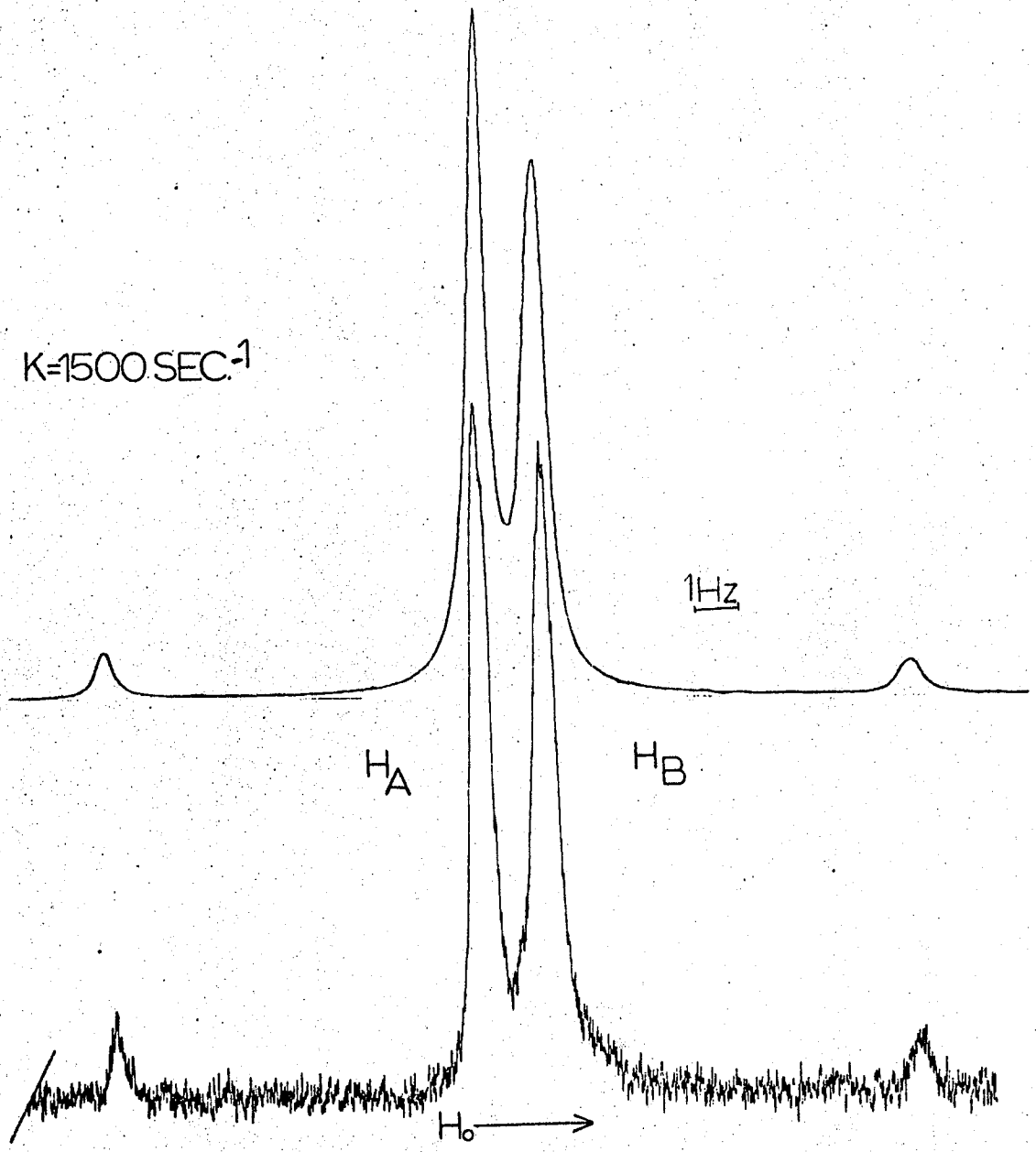
K=1500 SEC.-1
1Hz
H_A
H_B
H_o

Activation parameters were also calculated using the Arrhenius equation,

$$\log k = \frac{-E_a}{2.303R}\frac{1}{T} + \log A \qquad (4\text{-}11)$$

A plot of log k versus $\frac{1}{T}$ (see table X) gives a slope and intercept proportional to the energy of activation E_a and the frequency factor A. This plot is shown in figure 19, and the activation parameters are recorded in table XI. For purposes of comparison table XI includes the activation parameters for the hindered internal rotation of the dichloromethyl groups in α, α, α', α' - 2, 3, 5, 6 - octachloroxylene (OCX) (16) and in PCT (17,27).

A modified version of the energy plot calculated by Barber (16) is given in figure 20. His calculations which are based on modified Buckingham and/or van der Waals potential functions (39,40) do not make any allowances for the possibility of buttressing between ortho and meta chlorines and hence are not entirely representative of the rotation in 2, 3, 6 - PCT. Slight modifications to correct for the buttressing effects in 2, 3, 6 - PCT are suggested in figure 20 by broken lines. An explanation of these modifications will now be presented.

The small difference in free energy ($\Delta G^o \approx 50$ cal/mole) between the two conformations is believed to originate from the steric interactions between the ring and side-chain

FIGURE 18

Eyring plot of log k/T versus 1/T. The data plotted are found in table X.

$$\log (k/T) = (-2905 \pm 60)\ (1/T) + (8.49 \pm 0.21)$$

correlation coefficient = 0.9974.

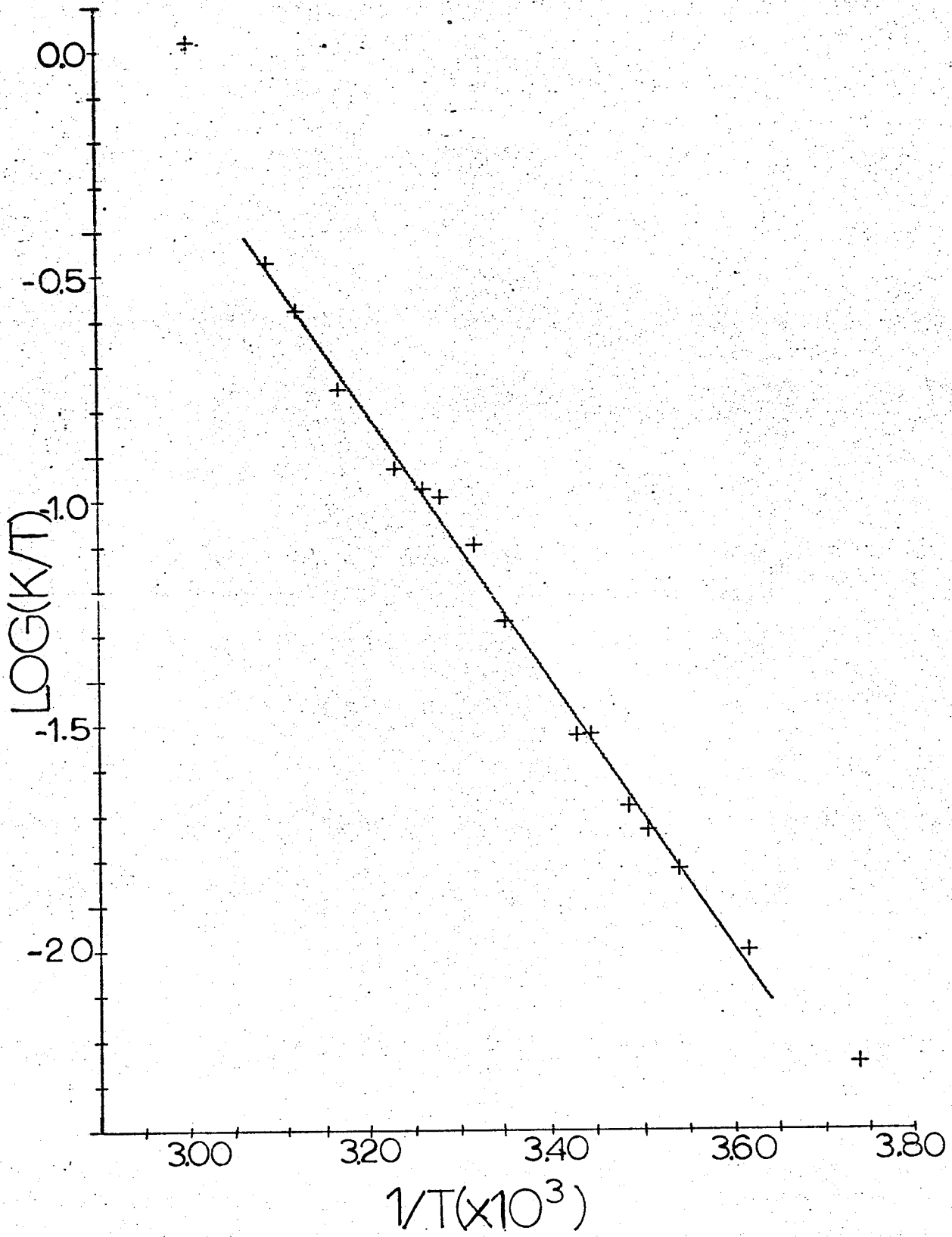
0.0
-0.5
-1.0
-1.5
-2.0
LOG(K/T)
3.00
3.20
3.40
3.60
3.80
1/T(X10³)

FIGURE 19

Arrhenius plot of log k versus 1/T. The data plotted are found in table X.

$$\log k = (-3010 \pm 60)\ 1/T + (11.40 \pm 0.21)$$

correlation coefficient = 0.9974

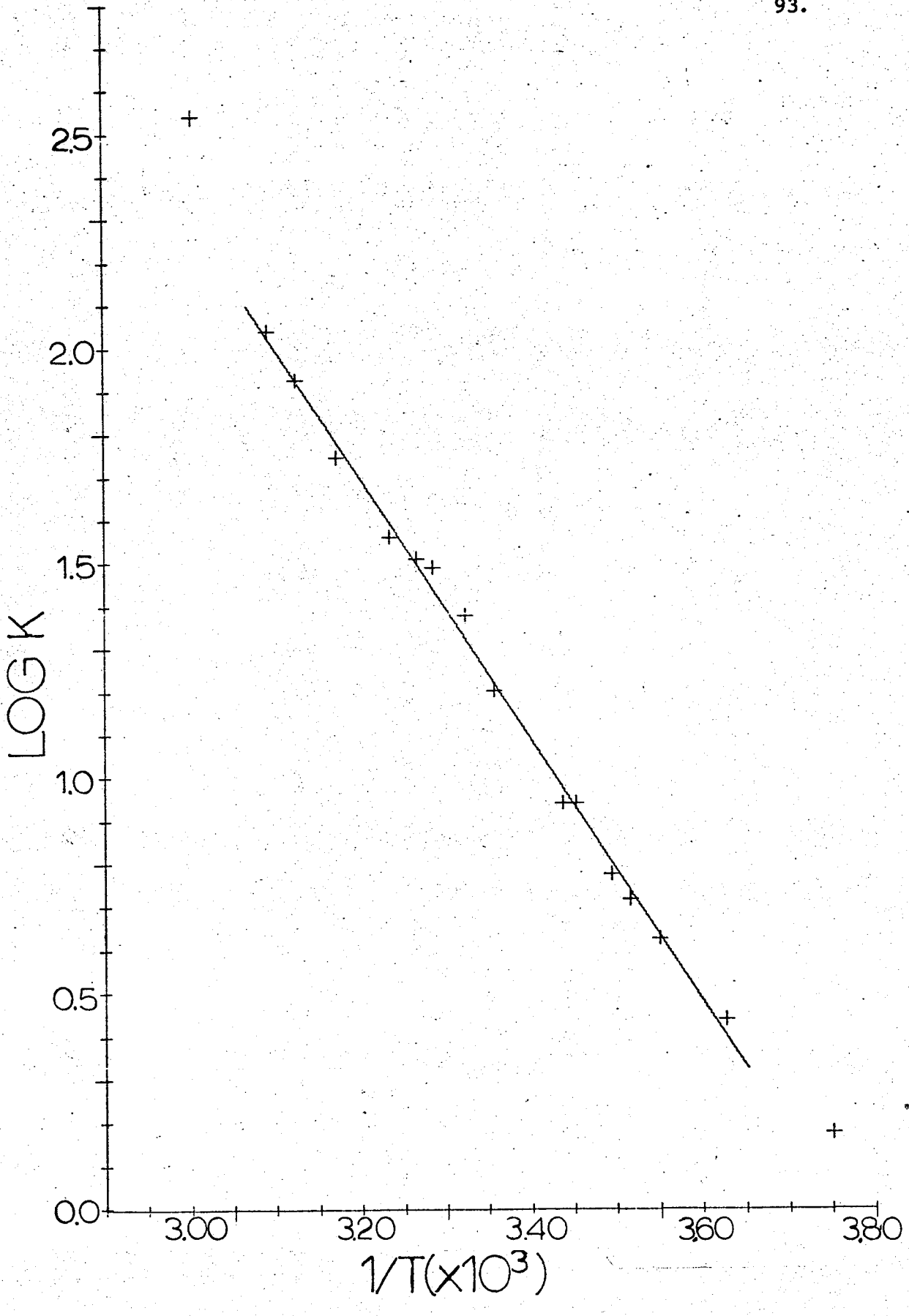
LOG K
2.5
2.0
1.5
1.0
0.5
0.0
3.00
3.20
3.40
3.60
3.80
1/T(x10³)

TABLE XI

Summary of the activation parameters found for 2,3,6-PCT in toluene-d_8, for OXC(16), and for PCT (17,27)

Compound	Solvent	ARRHENIUS PARAMETERS		TRANSITION STATE PARAMETERS		
		E_a(Kcal mole^{-1})	Log A	$\Delta H^{\neq}$(Kcal mole^{-1})	$\Delta S^{\neq}$(eu)	$\Delta G^{\neq}$(Kcal mole^{-1})
2,3,6-PCT*	Toluene-d_8	14.0±0.3	11.3±0.2	13.3±0.3	-7.0±0.7	15.4±0.1(298°K)
OCX	Toluene-d_8	13.6±0.4	11.3±0.3	13.1±0.4	-7.3±1.3	15.4±0.1(286°K)
PCT	Toluene-d_8	15.2±0.2	12.7±0.2	14.6±0.2	-1.1±0.7	14.9±0.1(304°K)
PCT	Methylcyclohexane	14.3±0.6	12.0±0.5	13.7±0.6	-4.4±2.2	15.0±0.2(304°K)
PCT	Carbon disulfide	14.2±0.3	11.9±0.2	13.7±0.3	-4.4±1.0	14.9±0.1(291°K)

* For 2,3,6-PCT the activation parameters correspond to the rate process from conformation I to conformation II.

FIGURE 20

A graphical representation of the free energy change for the hindered rotation in 2, 3, 6 - PCT.

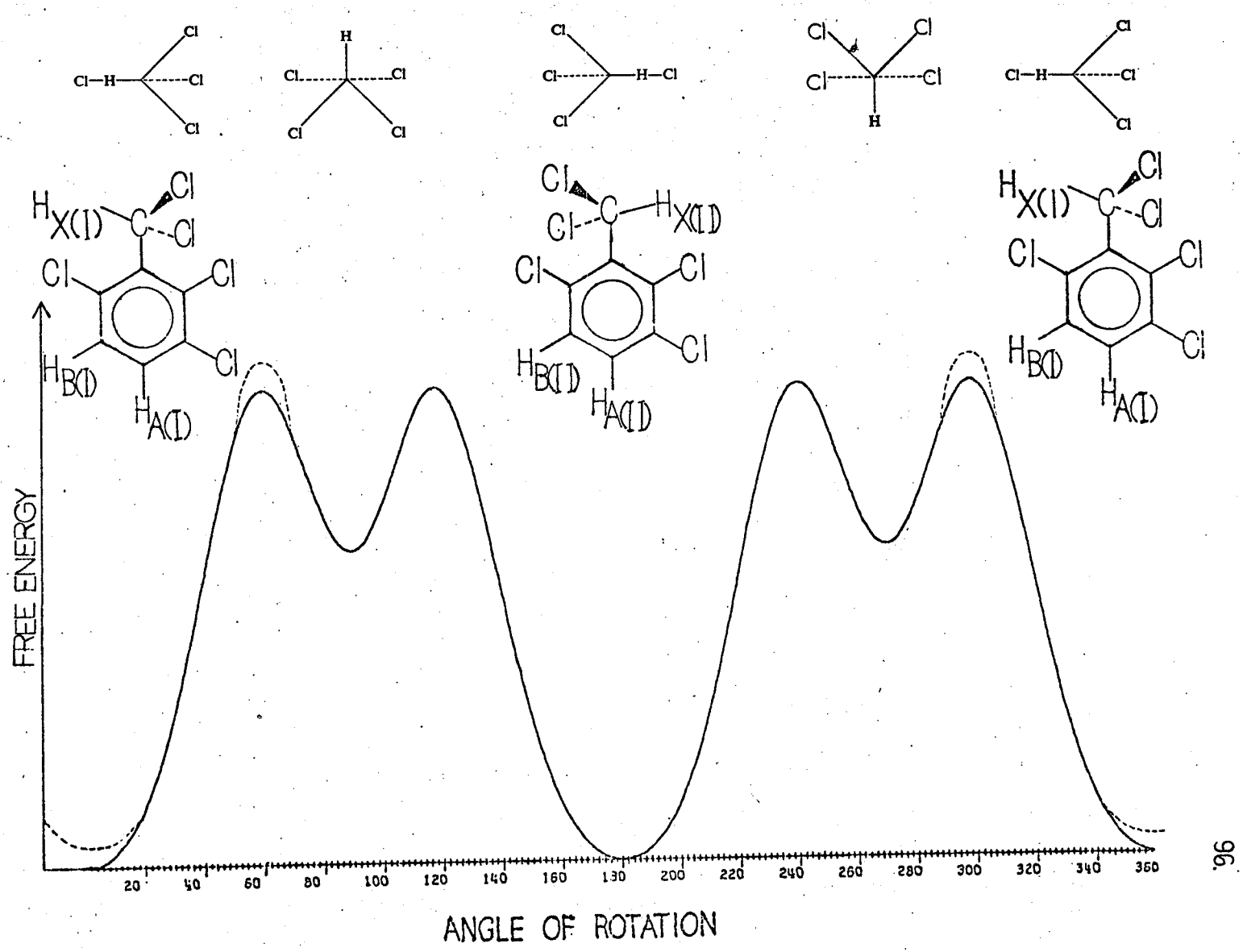
FREE ENERGY
20
40
60
80
100
120
140
160
180
200
220
240
260
280
300
320
340
360
ANGLE OF ROTATION

chlorines. In conformation I, the buttressing effect between the ortho and meta ring chlorines perhaps results in stronger interactions between the ring and side-chain chlorines. The absence of such an effect in conformation II presumably makes it more stable than conformation I.

At this point it is convenient to discuss the similarities between PCT, 2, 3, 6 - PCT and OCX. In a sense these three molecules form a series in which the buttressing effect steadily increases. It is noted that in PCT there is no buttressing effect, in 2, 3, 6 - PCT there is a buttressing effect in conformation I but not in conformation II, and in OCX the buttressing effect is present in both conformations of the dichloromethyl group. If it is assumed that the main contribution to the free energy diagram arises from the steric interactions between the ring and side-chain chlorines and that hydrogen bonding and other effects contribute much less, then the relative magnitude of ΔG^{o} and $\Delta G^{\neq}$ of the three molecules can easily be explained. The absence of buttressing in PCT and conformation II suggests that the ground state free energy of PCT and conformation II are comparable in magnitude. Similarly, the presence of the same type of buttressing in conformation I and OCX suggests that they have similar ground state free energies. This leads to the conclusion

that the ground state free energy of OCX is greater than that of PCT by an amount in the order of 100 cal/mole*.

As well it is evident that $\Delta G_I^{\neq}$ of 2, 3, 6 - PCT and $\Delta G_{OCX}^{\neq}$ should be very nearly equal since the buttressing is the same for both transition states. The data in table XI are consistent with this conclusion. ($\Delta G_I^{\neq} = \Delta G_{OCX}^{\neq} = 15.4 \pm 0.1$ Kcal/mole). Furthermore, because of the absence of buttressing in conformation II and PCT, $\Delta G_{II}^{\neq}$ and $\Delta G_{PCT}^{\neq}$ are expected to be of equal magnitude. Unfortunately there is no way of measuring $\Delta G_{II}^{\neq}$, but it seems logical to assign the same value for $\Delta G_{II}^{\neq}$ as for $\Delta G_{PCT}^{\neq}$. If this assumption is valid one can conclude that $\Delta G_{II}^{\neq}$ is less than $\Delta G_I^{\neq}$ by an amount equal to $\Delta G_{OCX}^{\neq} - \Delta G_{PCT}^{\neq} = 0.4 \pm 0.2$ Kcal/mole.

Table XI also shows similar values of $\Delta S^{\neq}$ for OCX and 2, 3, 6 - PCT but a more positive value for the entropy of activation for PCT. This difference may be again linked to the buttressing effect described previously. This effect increases the steric interactions more in the transition state than in the ground state. A net increase in steric

* Because there are two dichloromethyl groups in OCX the ground state free energy relative to that of PCT is approximately 2x50=100 cal/mole and not simply 50 cal/mole.

interactions in the transition state relative to the ground state is expected to decrease the number of degrees of freedom in the transition state and hence result in a negative $\Delta S^{\neq}$. Lack and Roberts (36) observe a similar effect on $\Delta S^{\neq}$ in their conformational studies.

3. Errors

The analysis of rate processes by the NMR complete line -shape method is frequently subject to large systematic errors (37,38). Such errors are more evident in the values for $\Delta S^{\neq}$, $\Delta H^{\neq}$ and E_a than in the value for $\Delta G^{\neq}$.

Saturation, excessive filtering and field inhomogeneities significantly distort the line-shapes and therefore must be avoided. Because the greatest changes in the line-shapes occur in the temperature range near the coalescence temperature, the data obtained from this range should be considered the most reliable.

The error introduced by the uncertainty in the value for the effective T_2 is relatively small in this rate study. The experimental spectra used for the determination for the rate constants were selected from the temperature range where the peaks are broad due to exchange. In this temperature range the contribution to the linewidth due to the effective T_2 is small in comparison to the contribution

due to exchange and hence the values obtained for the rate constants are quite accurate.

In a preceding section, the approximation that ΔH^{o} is constant with temperature was made. Were this not true, the values for the rate constants would be affected. Nevertheless, the size of the experimental error in the estimation of the rate constants is probably significantly larger than the magnitude of the error introduced by this approximation.

The transmission coefficient for the Eyring equation was assumed to have a value of ½. This appears to be a reasonable assumption providing the energy diagram is symmetrical about the transition state (34,35). Binsch suggests (4) that a value of 1 be used. However, only $\Delta S^{\neq}$ is affected by the value chosen for the transmission coefficient.

Finally, the error which is quoted for the activation parameters in table XI is determined from the standard error given by the least squares analysis of the data in table X.

G. Summary and Conclusions

A high resolution PMR investigation of the hindered internal rotation of the dichloromethyl group in 2, 3, 6 - PCT has been conducted using a complete line-shape computerized analysis of the experimental spectra. The study was carried out in a 20 mole % solution of 2, 3, 6 - PCT in toluene-d_8 over a temperature range from 254.6 to 378.2°K. The different peaks at the various temperatures were analyzed and assigned to the corresponding protons. Appropriate modifications for the different solvent shifts and populations were made in the treatment of the data.

The activation parameters for the rotational energy barrier were calculated in terms of the Arrhenius and the absolute reaction rate theories; they are recorded in table XI. Comparison of these results with those of similar molecules indicate similar energy barriers for the rotation of the dichloromethyl group in polysubstituted toluenes with chloro groups in the ortho position. The larger free energies of activation and smaller entropies of activation for 2, 3, 6 - PCT and OCX in comparison with the respective activation parameters for PCT were explained in terms of a buttressing effect between the meta and ortho chlorines in 2, 3, 6 - PCT and OCX. The same buttressing mechanism has also an effect on the difference in free

energy between the two conformations of PCT. This was measured by the difference in population and found to be 50±20 cal/mole. It is interesting and probably significant that the same buttressing effect increases $\Delta G^{\neq}$ by 0.4Kcal/mole (i.e. $\Delta G^{\neq}_{OCX} - \Delta G^{\neq}_{PCT} = 0.4$Kcal/mole) but increases the ground state free energy ΔG^{o} by only 50 cal/mole.

It is concluded that the main contribution to the energy barrier is steric hinderance between the chlorines.

H. Suggestions for Future Research

The results of this investigation could be checked by a repetition of the study using a 100 MHz spectrometer or a ^{13}C probe. This study suggests that the effects of the buttressing can be measured in three different ways:

1). By the relative stability of the conformations.

2). By the relative values of the activation parameters in PCT and OCX.

3). By the relative line positions of $\delta_{A(I)}$ compared to $\delta_{A(II)}$, $\delta_{B(I)}$ compared to $\delta_{B(II)}$ and $\delta_{X(I)}$ compared to $\delta_{X(II)}$.

Hence it should be possible to obtain a good measure of the steric interactions in polysubstituted benzenes by varying the substituents.

A study of the hindered rotation of a trichloromethyl group in a polysubstituted toluene would perhaps provide interesting results. With two halogens in the ortho positions, the most stable conformation would have two of the side-chain chlorines above the plane of the ring and the third below the plane. Consequently, the magnetic environment above and below the ring would be different. A group with protons out of the plane of the ring could detect this difference.

BIBLIOGRAPHY

1. C.S. Johnson Jr.,In "Advances in Magnetic Resonance", Vol.1, J.S. Waugh (Editor), Academic Press Inc., New York, 1965.

2. L.W. Reeves, In "Advances in Physical Organic Chemistry", Vol.3, V. Gold (Editor), Academic Press Inc., New York, 1965.

3. J.W. Emsley, J. Feeney and L.H. Sutcliffe, "High Resolution Nuclear Magnetic Resonance", Vol.1, Pergamon Press Ltd., Oxford, 1965.

4. G. Binsch, In "Topics in Stereochemistry", Vol. 3, E.L. Eliel and N.L. Allinger (Editors), John Wiley and Sons Inc., New York, 1968.

5. A. Carrington and A.D. McLachlan, "Introduction to Magnetic Resonance", Harper and Row, New York, 1967.

6. F. Bloch, Phys. Rev., 70, 460 (1946).

7. H.S. Gutowsky, D.W. McCall and C.P. Slichter, J. Chem. Phys., 21, 279 (1953).

8. H.S. Gutowsky, and A. Saika, J. Chem. Phys., 21, 1688 (1953).

9. H.S. Gutowsky and C.H. Holm, J. Chem. Phys., 25, 1228 (1956).

10. E.L. Hahn and D.E. Maxwell, Phys. Rev., 88, 1070 (1952).

11. H.M. McConnell, J. Chem. Phys., 28, 430 (1958).

12. J. Kaplan, J. Chem. Phys.,28, 278 (1958).

13. S. Alexander, J. Chem. Phys., 37, 967, 974 (1962).

14. G.M. Whitesides, Ph.D. Thesis, California Institute of Technology, 1964.

15. G. Binsch, J.Am. Chem. Soc., 91, 1304 (1969).

16. B. Barber,M.Sc. Thesis, University of Manitoba, 1970.

17. B. Fuhr,M.Sc. Thesis, University of Manitoba, 1969.

18. T. Schaefer, R. Schwenk, C.J. MacDonald, W.F. Reynolds, Can. J. Chem., 46, 2187 (1968).

19. B. Richardson and T. Schaefer, Can. J. Chem., 46, 2195 (1968).

20. R. Wasylishen and T. Schaefer, Can. J. Chem., 48, 0000 (1970).

21. R. Wasylishen, M.Sc. Thesis, University of Manitoba, 1970 .

22. G. Govil and H.J. Bernstein, J. Chem. Phys., 47, 2818 (1967).

23. G. Govil and H.J. Bernstein, J. Chem. Phys., 49, 911 (1968).

24. N. Davidson. "Statistical Mechanics", McGraw-Hill Book Co., Inc., New York, 1965.

25. K.I. Dahlqvist and S. Forsen, J. Phys. Chem., 49, 4062 (1965).

26. R.J. Abraham and M.A. Cooper, J. Chem. Soc., B, 202 (1967).

27. H. Gyulai, M.Sc. Thesis, University of Manitoba, 1970.

28. Z.M. Holubec and J. Jonas, J. Am. Chem. Soc., 90, 5986 (1968).

29. G. Binsch and J.D. Roberts, J. Am. Chem. Soc., 87 5157 (1965).

30. L.M. Jackman, T.E. Kavanaugh, and R.C. Haddon, Org. Mag. Res., 1, 109 (1969).

31. J. Peeling and T. Schaefer, Can. J. Chem., 48, 0000 (1970).

32. J.W. Emsley, J. Feeney, and L.H. Sutcliffe, "Progress in Nuclear Magnetic Resonance Spectroscopy", Vol. 3, Pergamon Press Ltd., Oxford, 1967.

33. R.J. Schwenk, M.Sc. Thesis, University of Manitoba, 1968.

34. W.F. Sheehan, Journal of Chemical Education, 47, 254 (1970).

35. D. Houalla, R. Wolf, D. Gagnaire, and J. Robert, Chem. Commun., 443 (1969).

36. R.E. Lack and J.D. Roberts, J. Am. Chem. Soc., 90 6997 (1968).

37. A. Allerhand, H.S. Gutowsky, J. Jonas and R.A. Meinzer, J. Am. Chem. Soc., 88, 3185 (1966).

38. A. Allerhand, F.M. Chen, and H.S. Gutowsky, J. Chem. Phys., 42, 3040 (1965).

39. R.A. Scott and H.A. Scheraga, J. Chem. Phys., 42, 2209 (1965).

40. K.E. Howlett, J. Chem. Soc., 1055 (1960).

41. R.A. Newmark and R.E. Graves, J. Phys. Chem., 72, 4299 (1968).